



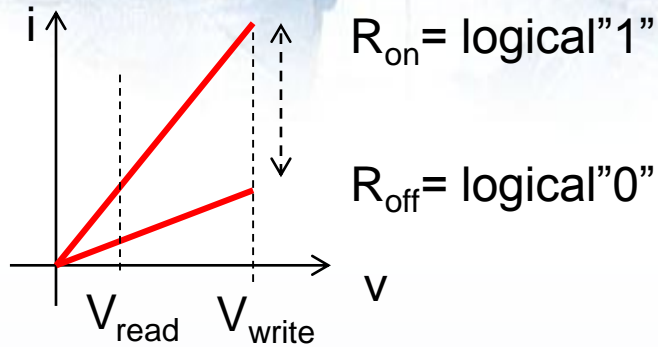
RRAM technology: From material physics to devices

Fabien ALIBART
IEMN-CNRS, Lille

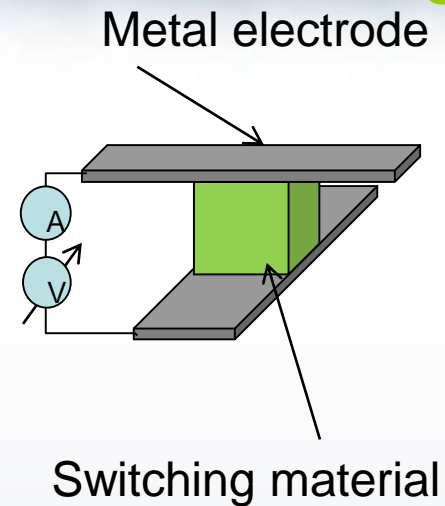
- Introduction: RRAM technology and applications
- Few examples:
 - Ferroelectric tunnel junction memory
 - Mott Insulator memory
 - Electro Chemical Memory (CB-RAM)
 - OxRAM
 - Valence Change Memory
 - Thermo Chemical Memory
- Conclusion: main challenges

RRAM: big picture

Principle of RRAM



- Induce a change of resistivity to discriminate two (or more) resistance states by electrical stress (1 bit of information, or more)
- Evaluate this state by a "Read" voltage, i.e. probing current
- Equivalent to a tunable resistor
- Non volatile



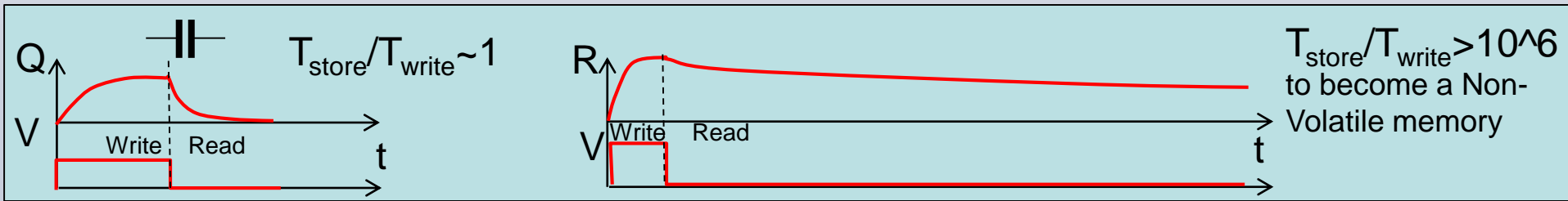
The time voltage dilemma

In other words: we want the write voltage V_{write} to be fast and to induce a large change of resistance and we want to be able to read for a very long time at V_{read} w/o changing the state: not trivial.

Whatever is the physical mechanism originating the change of resistance, we need

NON LINEARITY

Ex: the worst non-volatile memory
Storing charge on a capacitor



Some semantic...

There is today a debat around the proposition of memristance by HP in 2008.

$$v = \mathcal{R}(w)i$$

$$\frac{dw}{dt} = i$$

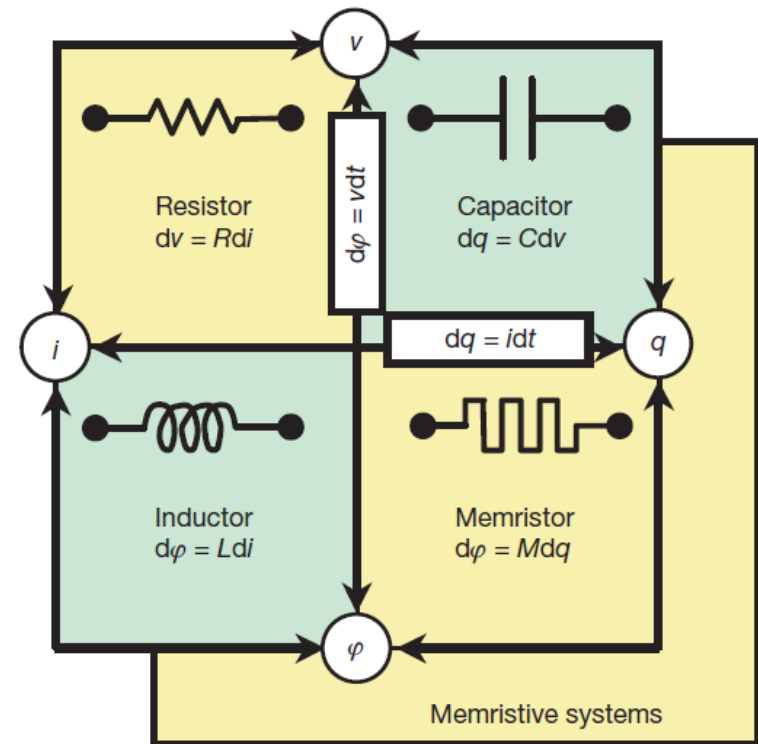
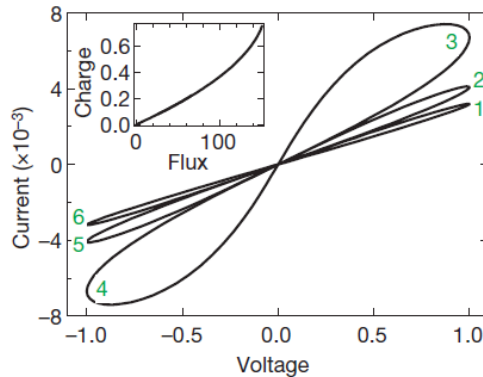


Figure 1 | The four fundamental two-terminal circuit elements: resistor, capacitor, inductor and memristor. Resistors and memristors are subsets of a more general class of dynamical devices, memristive systems. Note that R , C , L and M can be functions of the independent variable in their defining equations, yielding nonlinear elements. For example, a charge-controlled memristor is defined by a single-valued function $M(q)$.

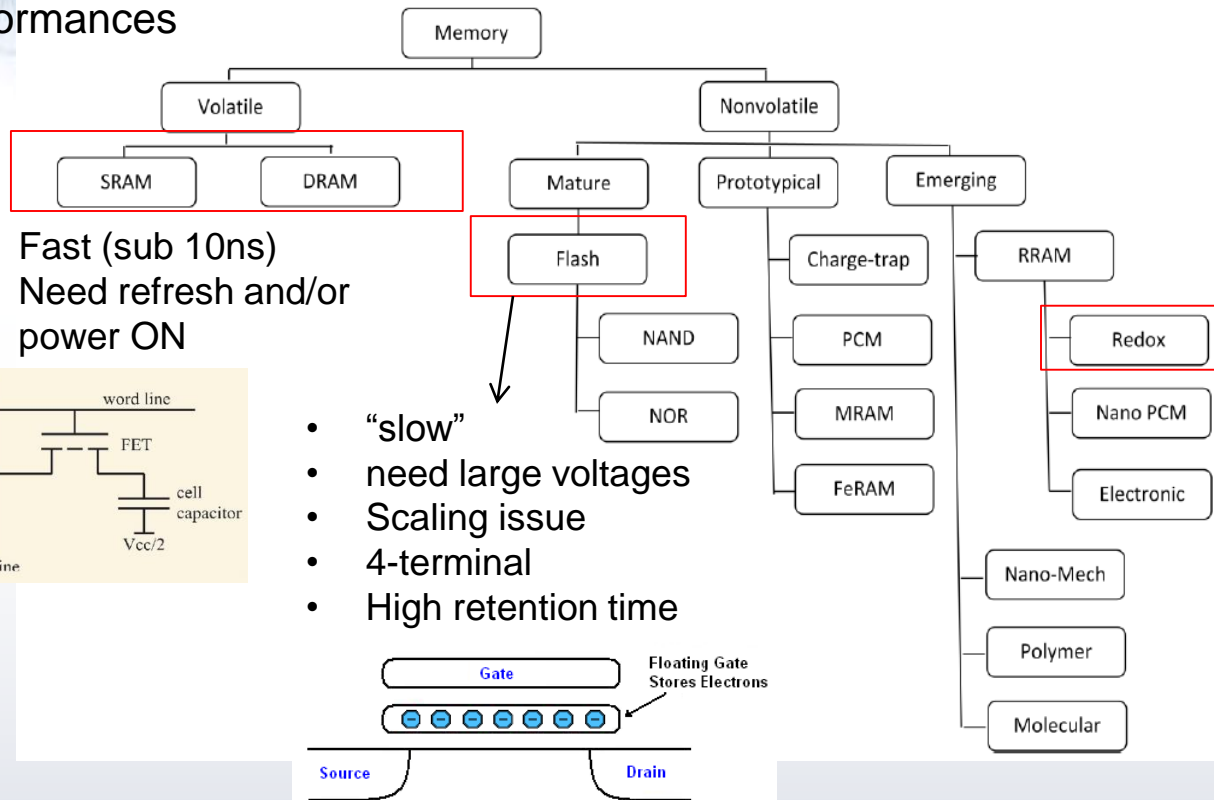
If we follow precisely the definition of memristor, none of the RRAM belongs to this class, but if we extend memrsitor to memristive devices, all RRAM can fit into this class...

“More or less the same, but not exactly similar...”

Classification under construction

The Holy grail: a universal memory

For RRAM to become a success story, it needs to bring more to industry, not only equivalent performances



- “slow”
- need large voltages
- Scaling issue
- 4-terminal
- High retention time

Try to do both with the same device:

- Fast (<10ns)
- Low switching energy (pJ)
- Non-volatile (10 year@85C)
- Reliable
- High endurance (up to 10^{12} cycles)

And more...

- Sub 10 nm integration
- New computing solution
- Multi-bit

Table 1 | Comparison of memory and storage technologies¹¹⁹. Note that circuit-level overheads for the listed performance metrics are in general different among different device technologies and could often dominate individual device performance.*

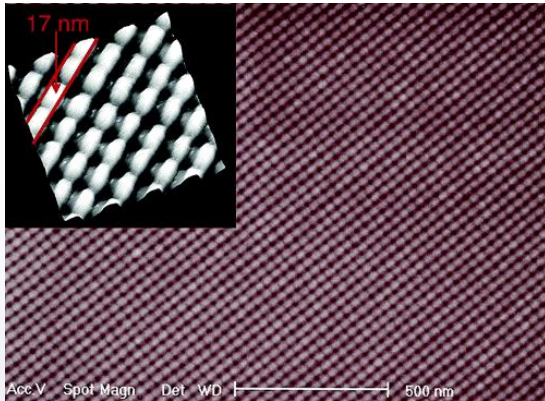
| | Memristor | PCM | STTRAM | SRAM | DRAM | Flash (NAND) | HDD |
|--------------------------------------|------------------|-----------------|------------------|----------------------------|-------------------|-----------------------------|------------------------|
| | | | Prototypes | | | Commercialized technologies | |
| Reciprocal density (F ²) | <4 | 4-16 | 20-60 | 140 | 6-12 | 1-4 [†] | 2/3 |
| Energy per bit (pJ) | 0.1-3 | 2-25 | 0.1-2.5 | 0.0005 | 0.005 | 0.00002 | 1-10 × 10 ⁹ |
| Read time (ns) | <10 | 10-50 | 10-35 | 0.1-0.3 | 10 | 100,000 | 5-8 × 10 ⁶ |
| Write time (ns) | ~10 | 50-500 | 10-90 | 0.1-0.3 | 10 | 100,000 | 5-8 × 10 ⁶ |
| Retention | years | years | years | As long as voltage applied | <<second | years | years |
| Endurance (cycles) | 10 ¹² | 10 ⁹ | 10 ¹⁵ | >10 ¹⁶ | >10 ¹⁶ | 10 ⁴ | 10 ⁴ |

*The energy to operate NAND Flash is typically hundreds of picojoules per bit primarily because accessing the memory cells requires charging word and bit lines to high voltages. [†]Smaller number represents an effective area for multi-level cells. PCM, phase-change memory; STTRAM, spin torque transfer random access memory; SRAM, static RAM; DRAM, dynamic RAM; HDD, hard disk drive.

RRAM potential

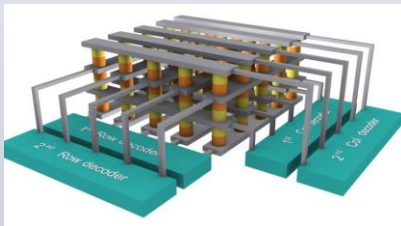
PROS and CONS

- Wide range of material systems (many CMOS compatible) and physical phenomena
- High density due to lateral scaling and ..

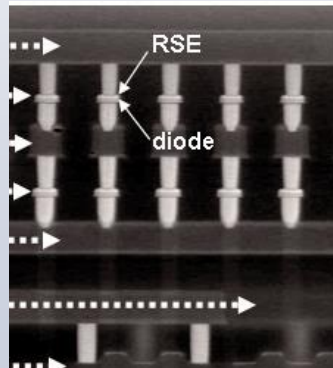


HPLab,
2005

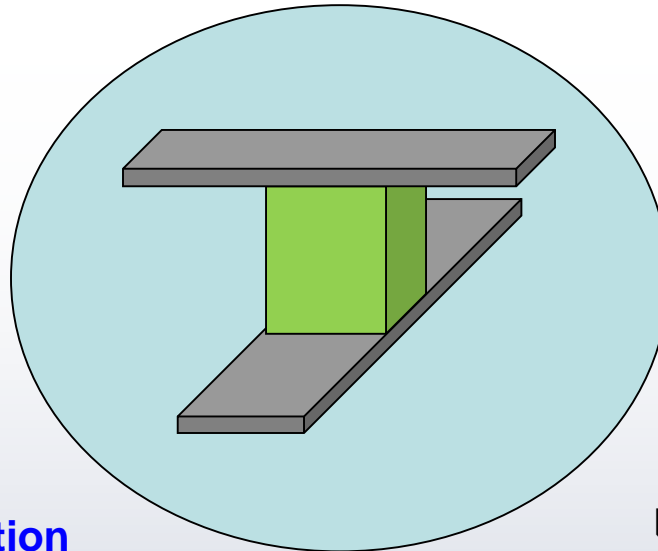
... monolithical 3D integration



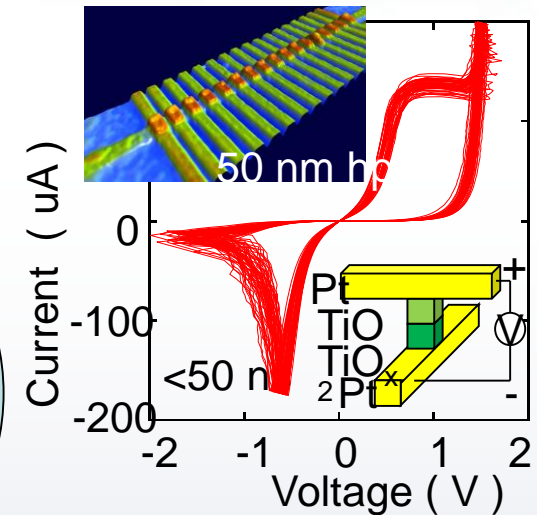
M.-J.Lee et al. *IEDM*
85 (2008)



Kawahara et al. Samsung,
2012

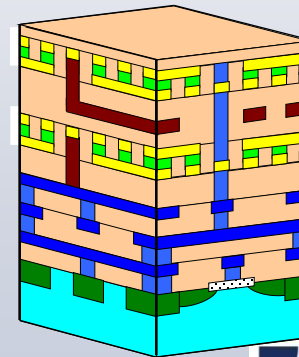


- but simple functionality



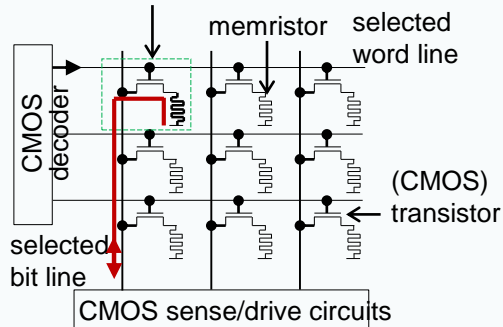
J. Yang et al. *Nature Nano*,
(2008)

- Solution: hybrid circuits

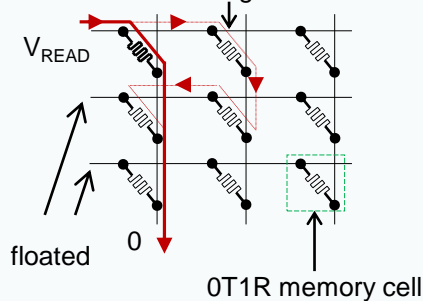


crossbar add-on
with integrated
memristive
devices
CMOS circuits

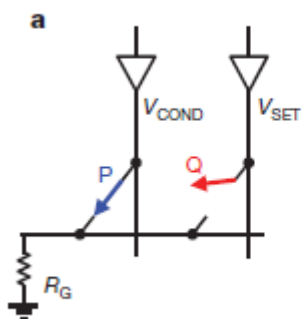
1transistor/1resistor(1T1R)
memory cell



READ OPERATION
leakage current



LOGIC
(HPLab, Nature)

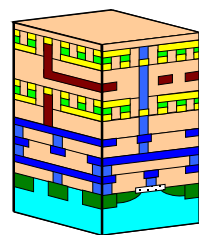


$q' \leftarrow pIMPq$

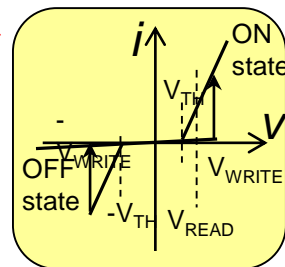
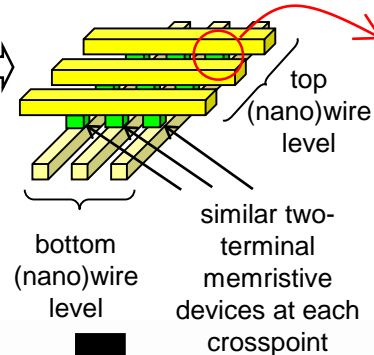
| In | In | Out |
|-----|-----|------|
| p | q | q' |
| 0 | 0 | 1 |
| 0 | 1 | 1 |
| 1 | 0 | 0 |
| 1 | 1 | 1 |

Killer Applications

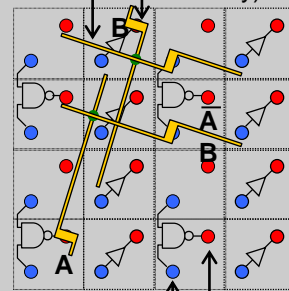
HYBRID CIRCUITS



crossbar add-on
with integrated
memristive
devices
conventional
complementary
metal oxide
semiconductor
(CMOS) circuits

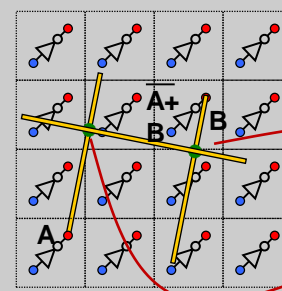


crossbar wires (only few
are shown for clarity)

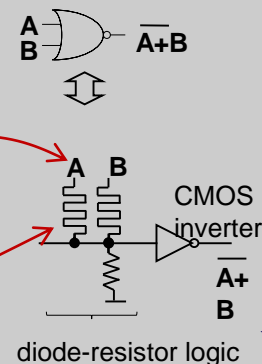


CMOS cell
vias connecting
CMOS and crossbar
wires

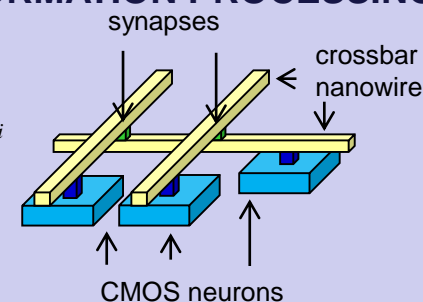
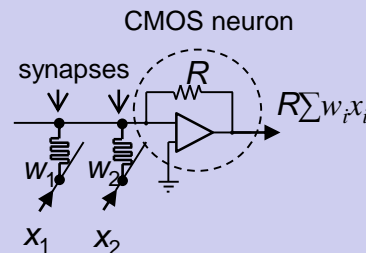
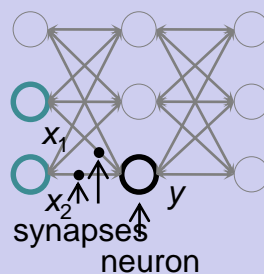
FPGA



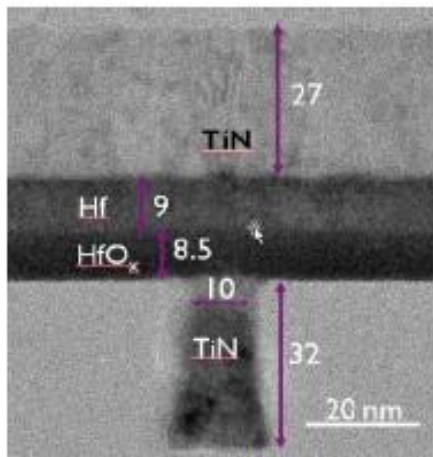
CMOS cell
diode-like
memristors



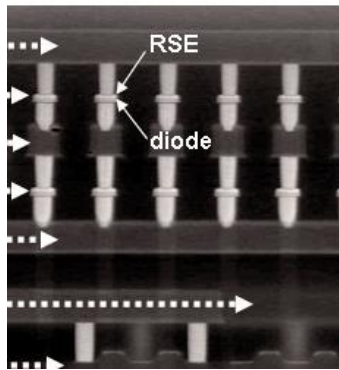
BIO-INSPIRED AND MIXED-SIGNAL INFORMATION PROCESSING



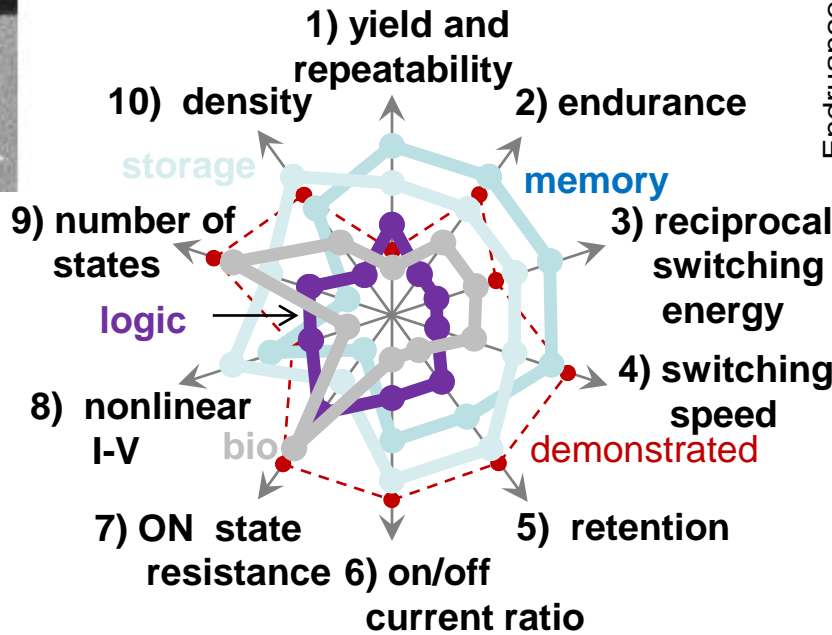
State-of-the-Art Performance



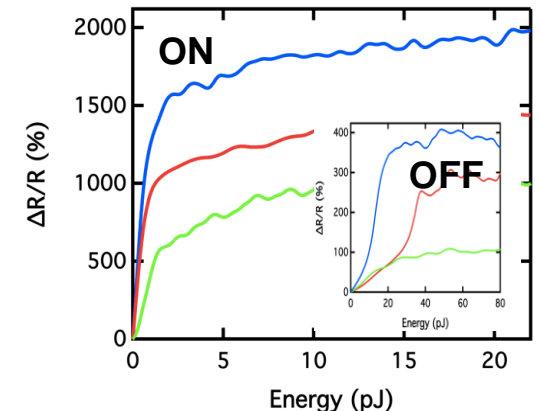
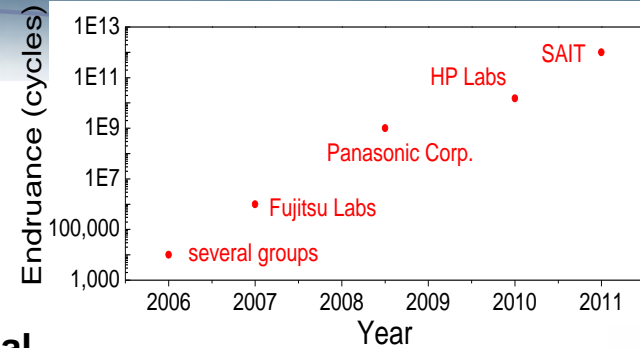
Govoreanu, et al IEDM, 2012



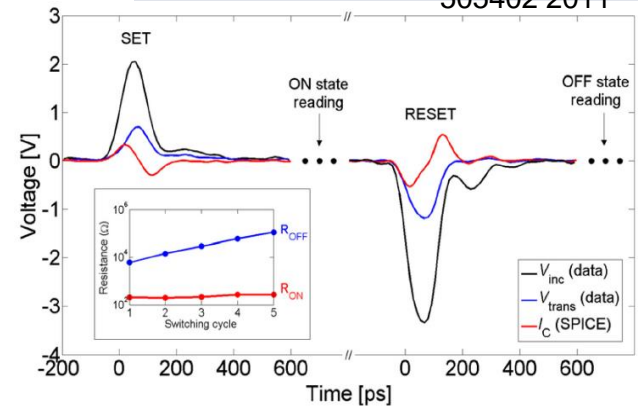
Kawahara et al. Samsung, 2012



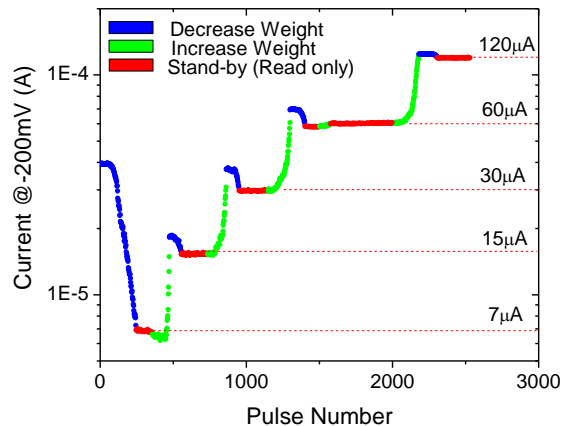
J. Yang and D. Strukov (Nature Nano 2013)



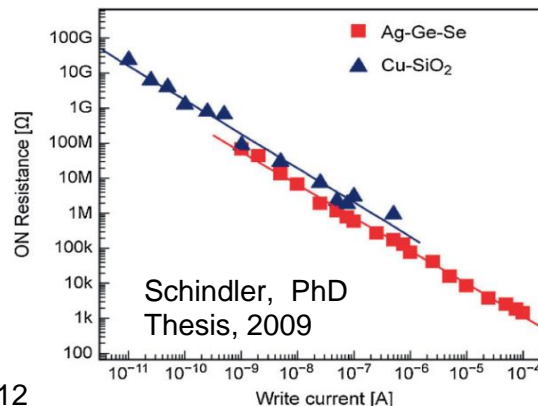
Strachan et al, Nanotechnology, 22, 505402 2011



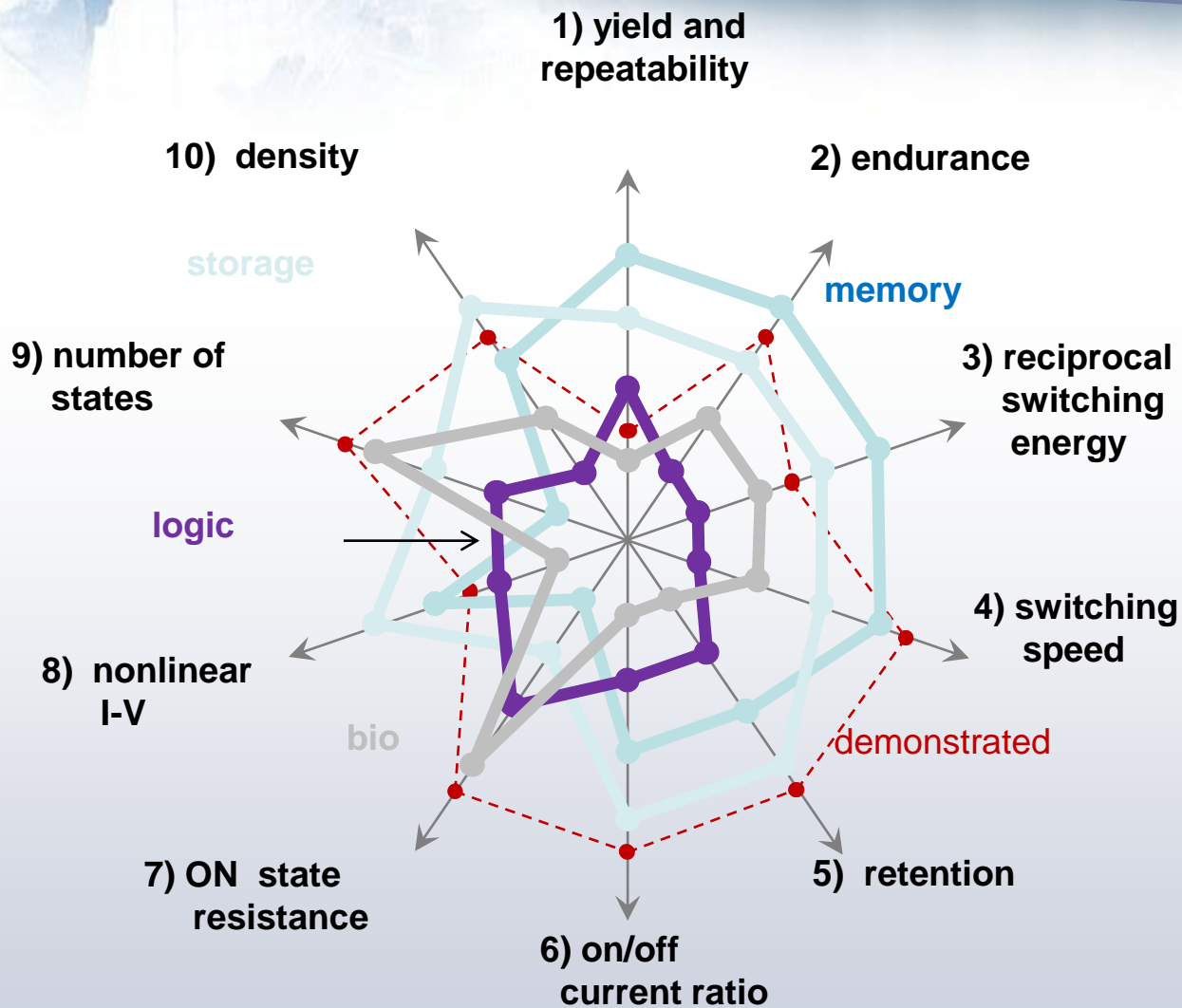
Torrezan et al, Nanotechnology, 22, 485203 2011



Alibart et al, Nanotechnology, 23, 074508, 2012

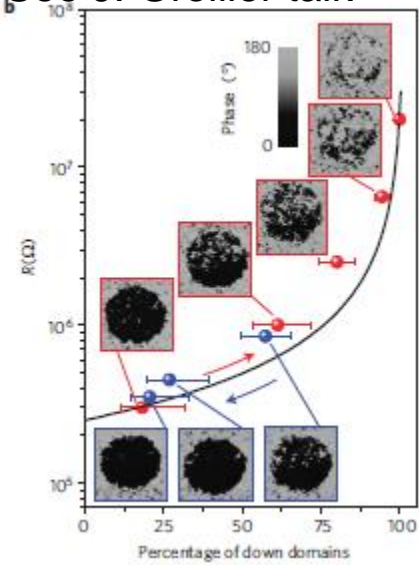


Schindler, PhD Thesis, 2009



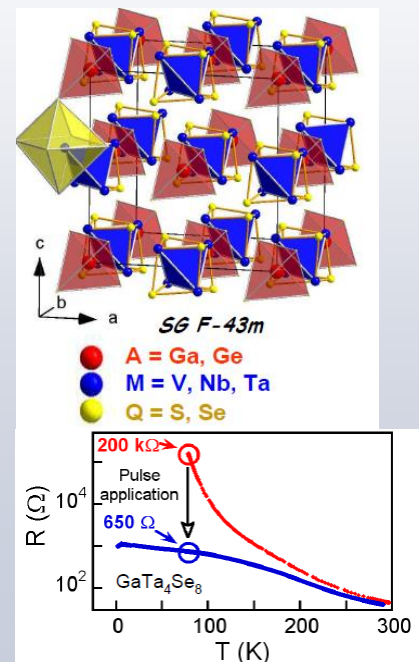
RRAM technologies

See J. Grollier talk

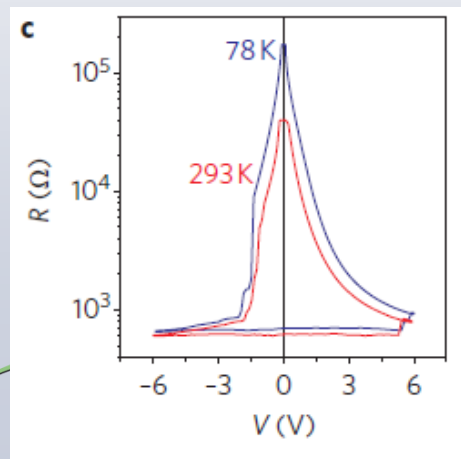


Mott transition

See J. Tranchant (IMN) talk



Chen-NatNano2012
Anderson localisation tuning
in SiO₂_Pt/NPs films



Resistive Switching

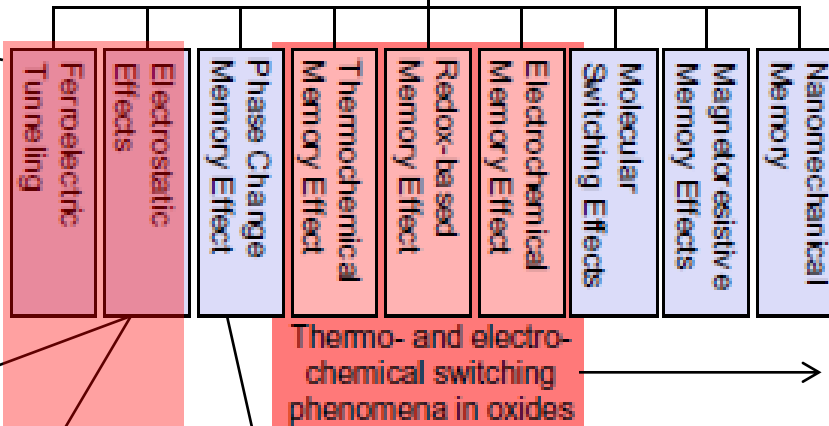
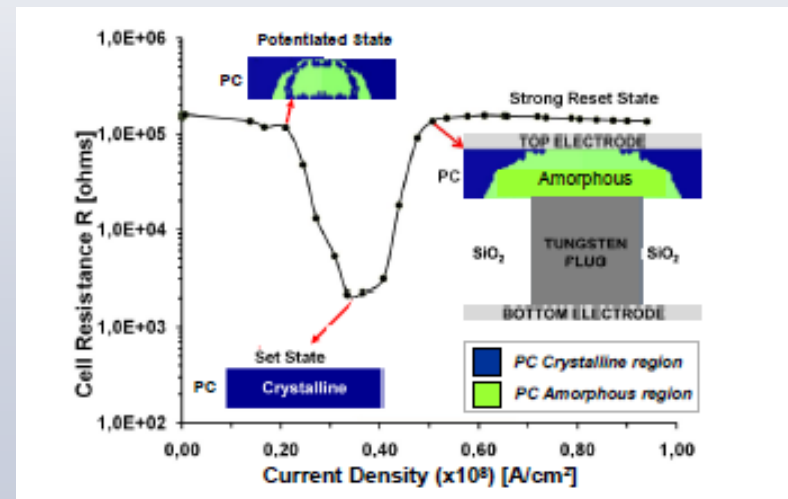


Fig. 1. Emerging memories – classification of the resistive switching mechanisms.

→ This review

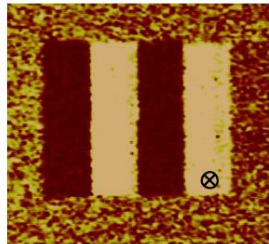
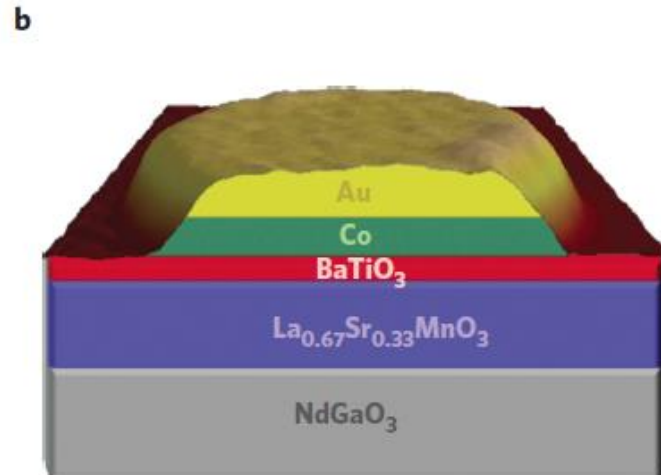
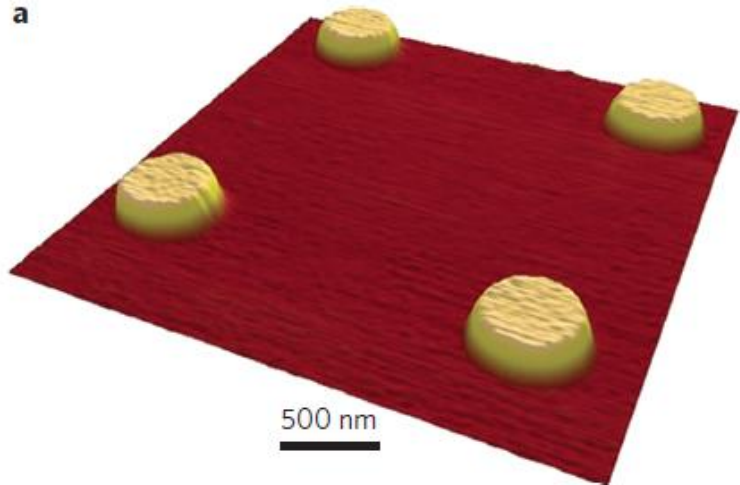
Thermally-induced phase change



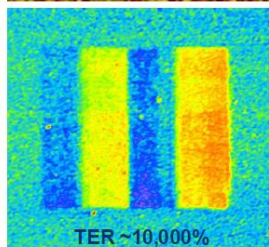
FeRAM

Work from UMPHys-Thales (Paris)

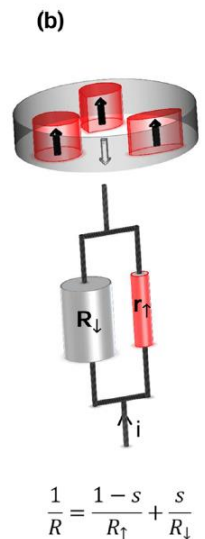
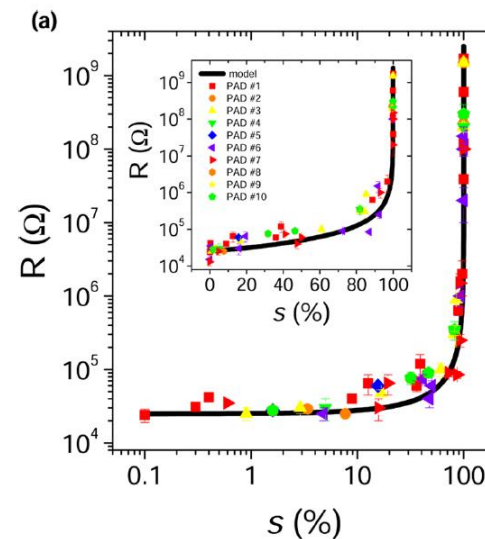
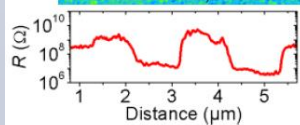
Change of resistivity is associated to the change of polarization of a ferroelectric thin film



PFM analysis of domains reversal via electric field stress



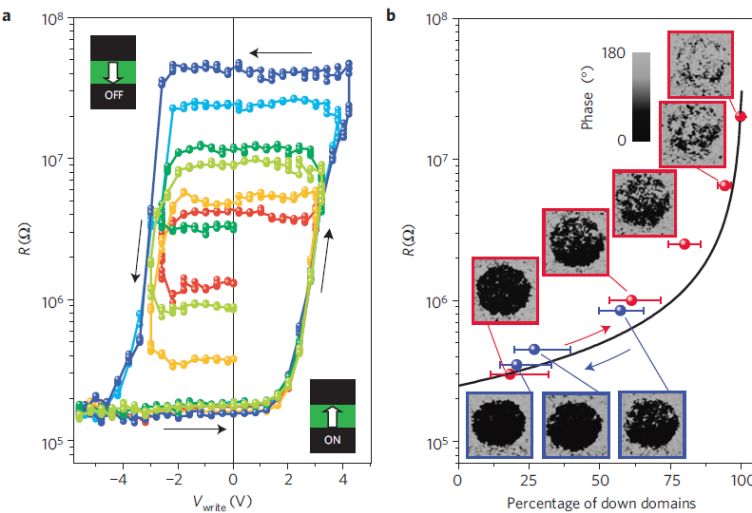
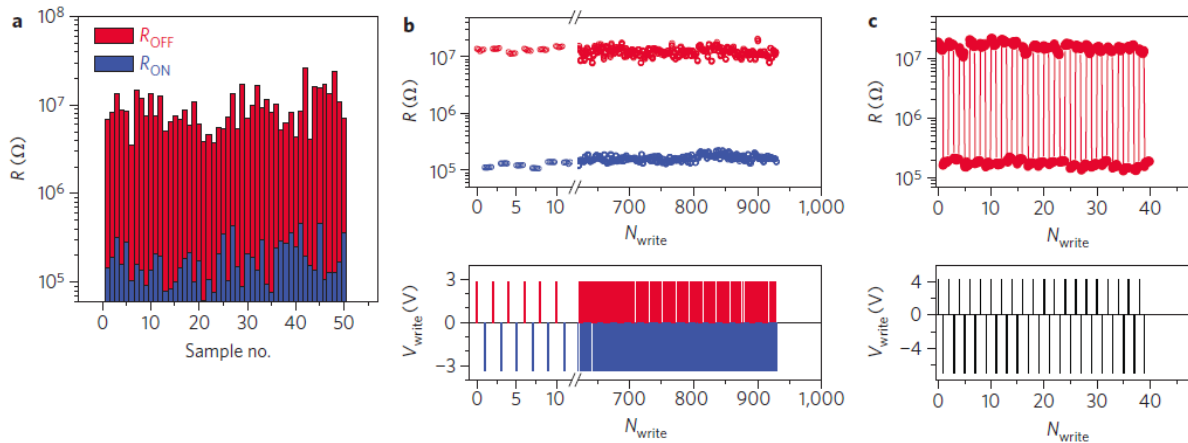
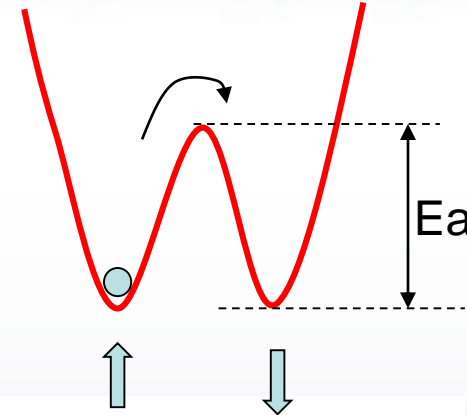
Polarization -> change of band alignment -> change of resistivity



FeRAM

Non-linearity:

$$\text{Exp}(E_a/kT) \gg \text{Exp}(qV/kT)$$

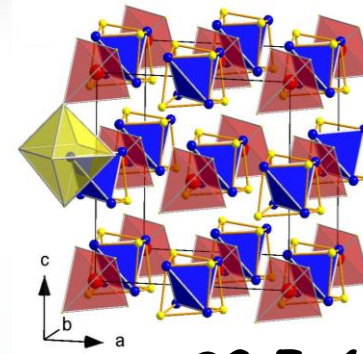
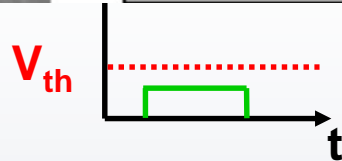
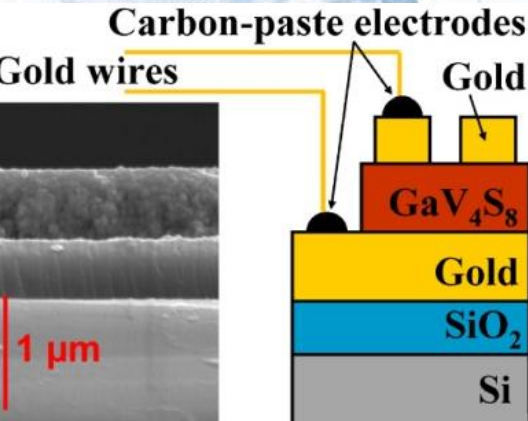


| | Volatile | | Non-volatile | | | | | |
|-------------------|---------------------|----------------------------------|-------------------------|----------------------------------|----------------------------|------------------|------------------------------|----------------------------|
| | DRAM | SRAM | NAND Flash | Trapping charge | FeRAM | MRAM | PCM | FTRAM |
| Storage mechanism | Charge on capacitor | Interlocked state of logic gates | Charge on floating gate | Charge trapped in gate insulator | Ferroelectric polarization | Magnetization | Amorphous/crystalline phases | Ferroelectric polarization |
| Cell elements | 1T1C | 6T | 1T | 1T | 1T1C | 1(2)T1C | 1T1R | 1T1R |
| Feature size (nm) | 50 | 65 | 90 | 50 | 180 | 130 | 65 | 50 |
| Cell area | 6F ² | 140F ² | 5F ² | 6F ² | 22F ² | 45F ² | 16F ² | 4F ² |
| W/E time | <10 ns | 0.3 ns | 0.1 ms | 20 μs | 10 ns | 20 ns | 50 ns | 10 ns |
| Retention time | 64 ms | 0 | > 10 y | > 10 y | > 10 y | > 10 y | > 10 y | > 5 days |
| Write cycles | >1E16 | >1E16 | >1E5 | >1E5 | 1.00E+14 | >1E16 | 1.00E+09 | >900 |
| Write voltage | 2.5 | 2.5 | 15 | 8 | 0.9-3.3 | 1.5 | 3 | 3 |
| Read voltage | 1.8 | 1 | 2 | 1.6 | 0.9-3.3 | 1.5 | 3 | 0.1-1 |
| Write energy | 5 fj | 0.7 fj | 10 fj | 100 fj | 30 fj | 100 pj | 6 pj | <10fj |

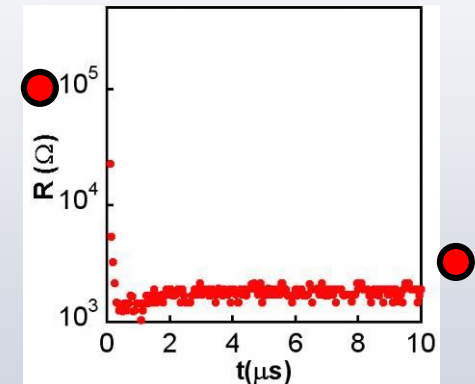
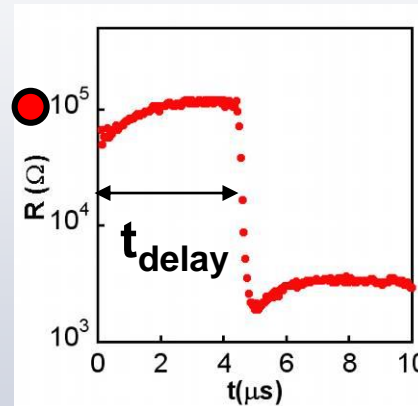
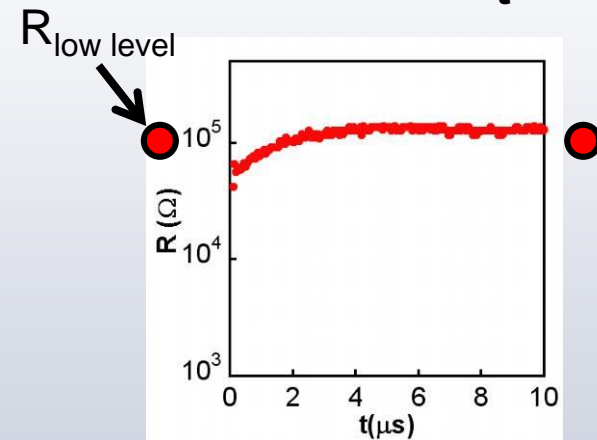
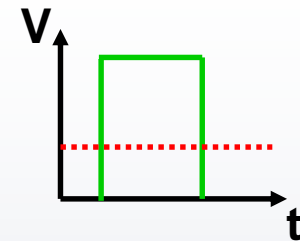
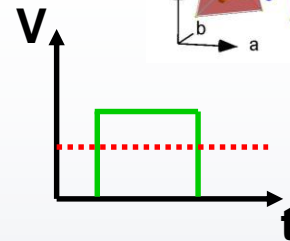
Next big challenge:

- Integration with CMOS friendly materials

Clustered lacunar spinel structure :



SG F-43m



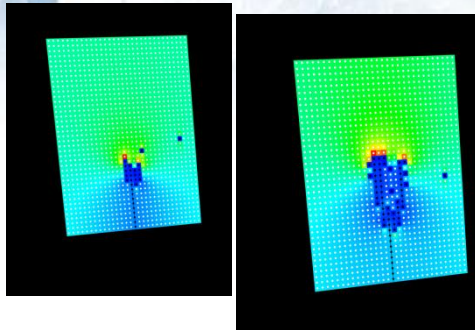
✓ no transition

✓ volatile
Resistive switching

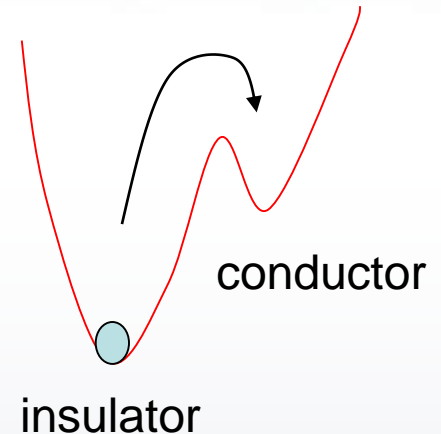
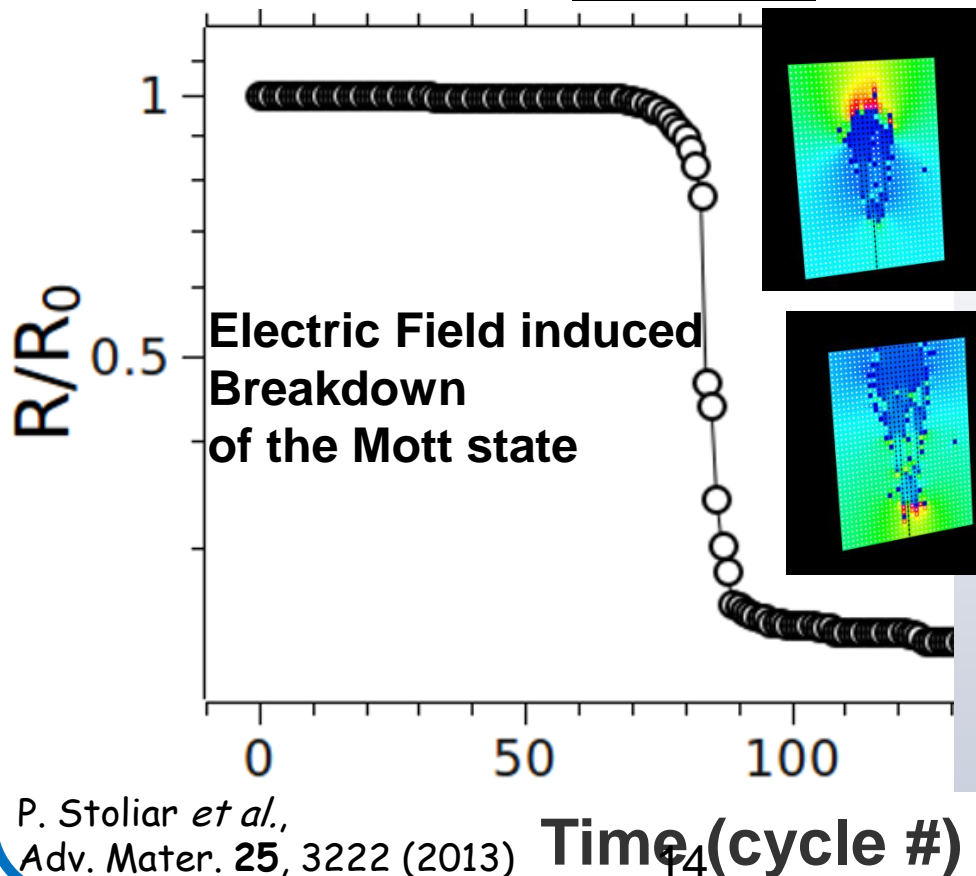
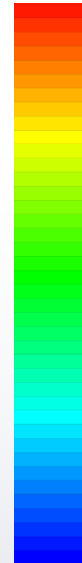
✓ fast non-volatile
Resistive switching

Modeling of the volatile resistive switching

Model



Electric Field



Metastable ON state
-> OFF state more stable
(volatile transition)
BUT domain size effect
that induces a non-
volatile transition

P. Stolar *et al.*,
Adv. Mater. **25**, 3222 (2013)

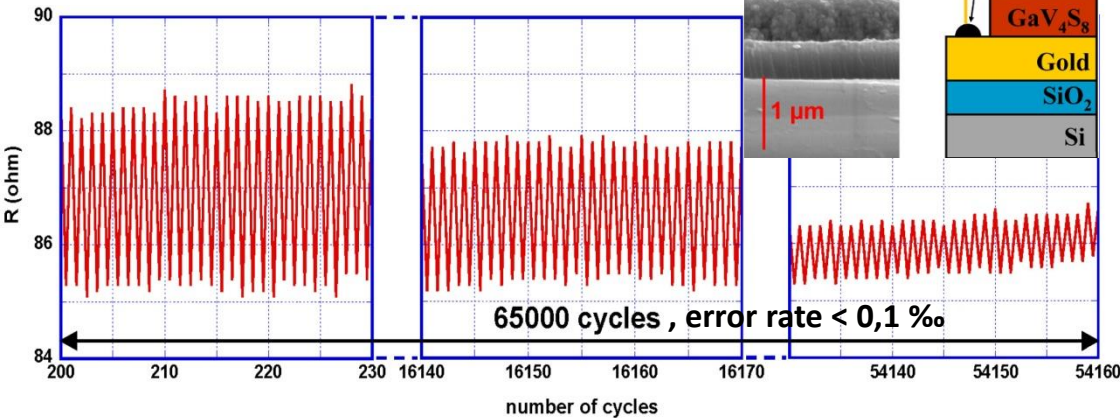
14
Time (cycle #)

V. Guiot *et al.*,
Nature Comm; **4**, 1722 (2013)

Electrical performances of GaV_4S_8 for Mott memories

Resistive switch cycling endurance

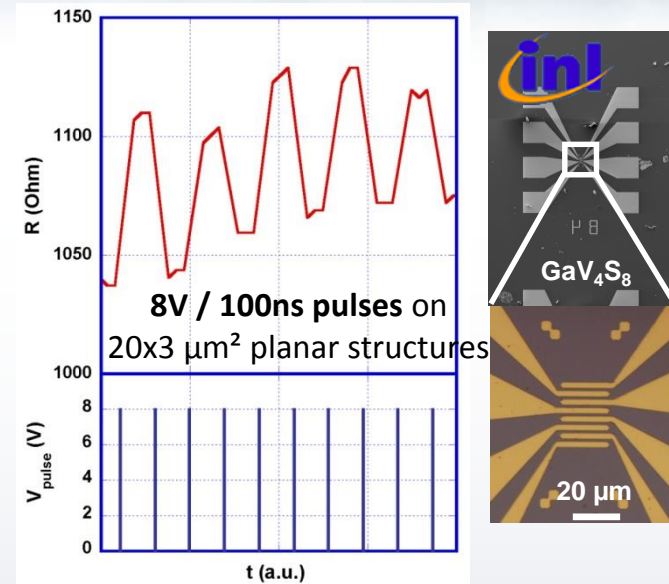
2V / 1ms pulses on $50 \times 50 \mu\text{m}^2$ MIM structures



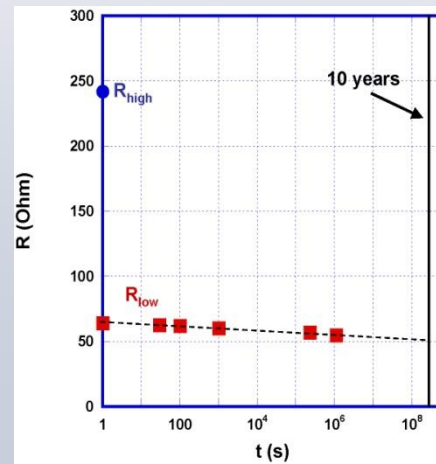
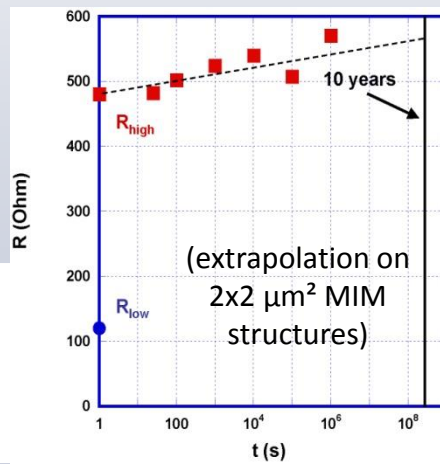
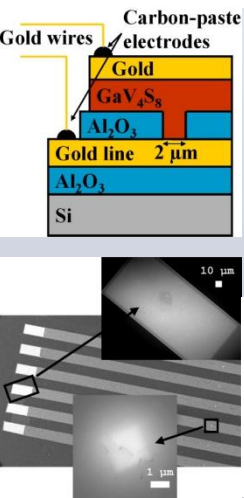
+ writing / erasing
voltage $\leq 2\text{V}$

J. Tranchant et al. Thin Solid Films, 533 (2013) 61

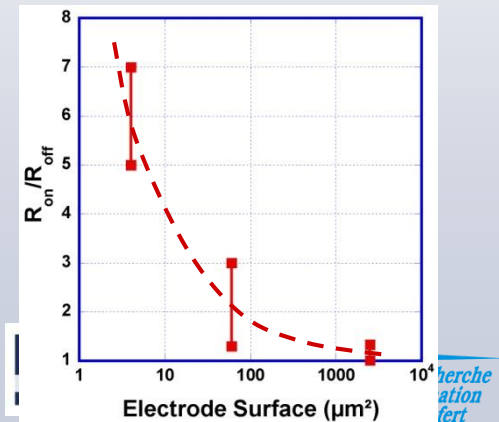
Writing / erasing times $\leq 100 \text{ ns}$



Data retention : high and low resistance states > 10 years



Increase of $R_{\text{on}}/R_{\text{off}}$ with downscaling



Electrochemical Cell

- Other names:
 - Solid state electrolyte memory
 - Conductive bridge memory
 - Programmable metallization cell



Solid state electrolyte with
host ions M^{Z+} ions

Active Electrode (e.g. Ag_2S , Cu_2S , $RbAg_4I_5$)
(e.g., Ag, Cu)

or
insulator doped with M^{Z+}
(e.g. SiO_2 , WO_2 , GeS ,
 $GeSe$)

Counter Electrode
(e.g., Pt, Ir, Au, W)

typically amorphous or
crystalline

| Electrolytes | Bottom Electrode | Top electrode | Switching mode | reference |
|--------------------------------------|-----------------------------------------------------------------------|-------------------------|----------------|-----------|
| Sulfides: | | | | |
| Ge_xS_x | W | Ag | Bipolar | 55 |
| As_2S_3 | Au | Ag | Bipolar | 56 |
| Cu_2S | Cu | Pt | Bipolar | 57, 58 |
| $\text{Zn}_x\text{Cd}_{1-x}\text{S}$ | Pt | Ag | Bipolar | 59 |
| Iodides: | | | | |
| AgI | Pt | Ag | Bipolar | 60 |
| RbAg_4I_5 | Pt | Ag | Bipolar | 61 |
| Selenides: | | | | |
| Ge_xSe_y | W | Ag, Cu | Bipolar | 62 |
| Tellurides: | | | | |
| Ge_xTe_y | TiW | Ag | Bipolar | 63 |
| Ternary chalcogenides: | | | | |
| Ge-Sb-Te | Mo | Au, Ag | Bipolar | 64 |
| oxides | | | | |
| Ta_2O_5 | Pt | Cu | Bipolar | 65 |
| SiO_2 | W | Cu | Uni/Bipolar | 66 |
| HfO_2 | Pt | Cu | Bipolar | 67 |
| WO_3 | Pt | Cu | Bipolar | 68 |
| ZrO_2 | Ag | Au | Bipolar | 69 |
| SrTiO_3 | Pt | Ag | Bipolar | 70 |
| TiO_2 | Pt | Ag | Bipolar | 71 |
| CuO_x | Cu | Al | Unipolar | 72 |
| ZnO | Pt, Al doped ZnO | Cu | Bipolar | 73 |
| Al_2O_3 | Al | Cu | Bipolar | 74 |
| MoO_x | Cu | Pt | Bipolar | 75 |
| GdO_x | Pt | Cu doped MoO_x | | 76 |
| Others: | | | | |
| MSQ | Pt | Ag | Bipolar | 77 |
| doped organic semiconductors | Pt | Cu | Bipolar | 78 |
| nitrides | Pt | Cu | Bipolar | 79 |
| amorphous Si | $\text{P}^+\text{-Si}$ | Ag | Bipolar | 80 |
| Carbon | Pt | Cu | Bipolar | 81 |
| vacuum gaps | $\text{RbAg}_4\text{I}_5/\text{Ag}$, $\text{Ag}_2\text{S}/\text{Ag}$ | W, Pt | Bipolar | 82, 83 |

Typical I-V and Process Cartoon

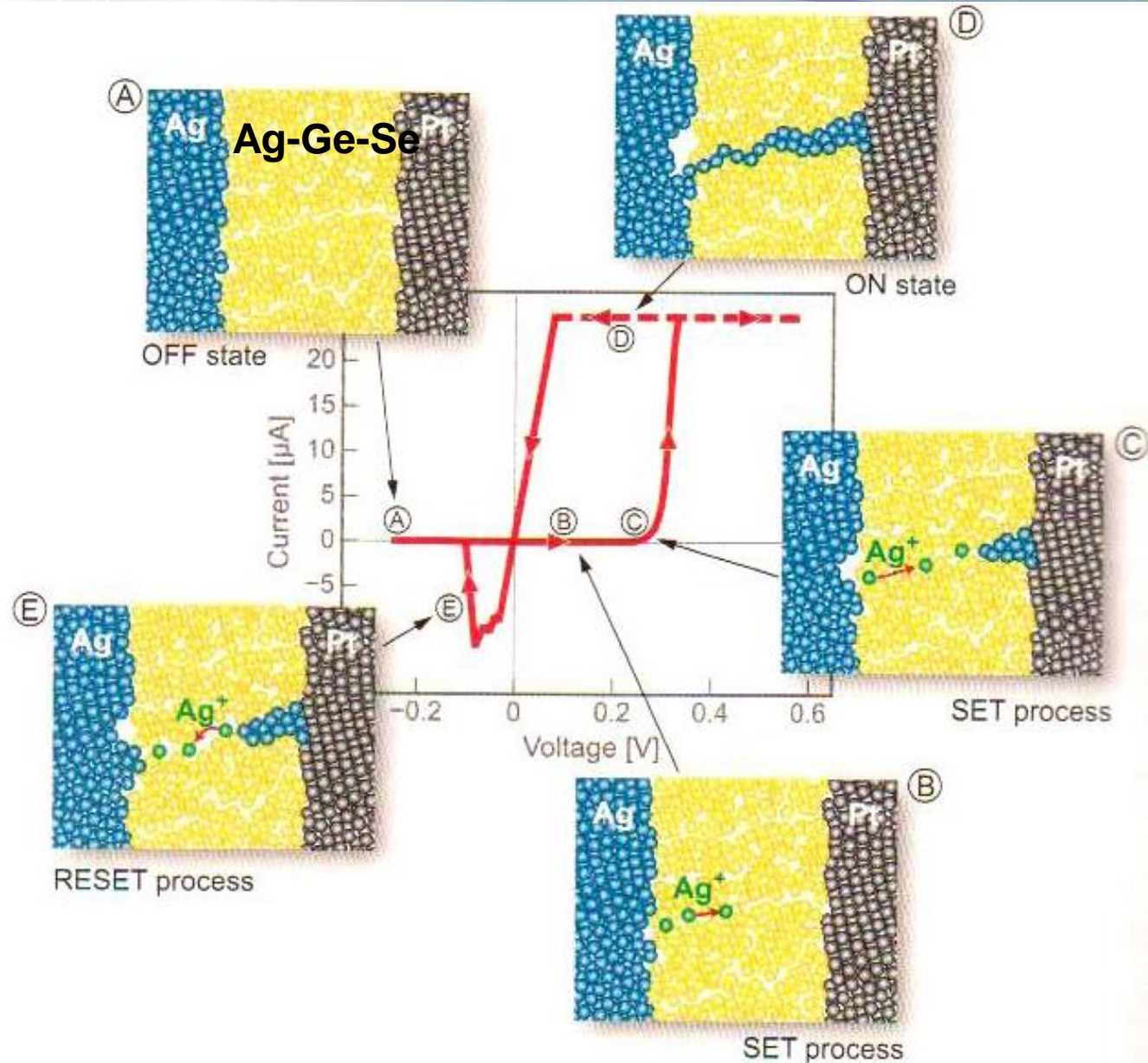
(A) OFF state

(B, C) SET process:

(i) Ag oxidized to Ag^+ ; (ii) drift in electric field ; (iii) reduced and electro-crystallized

(D) SET process:
complete bridging
(compliance-related)

(E) RESET process:
opposite of SET
(heat assisted?)

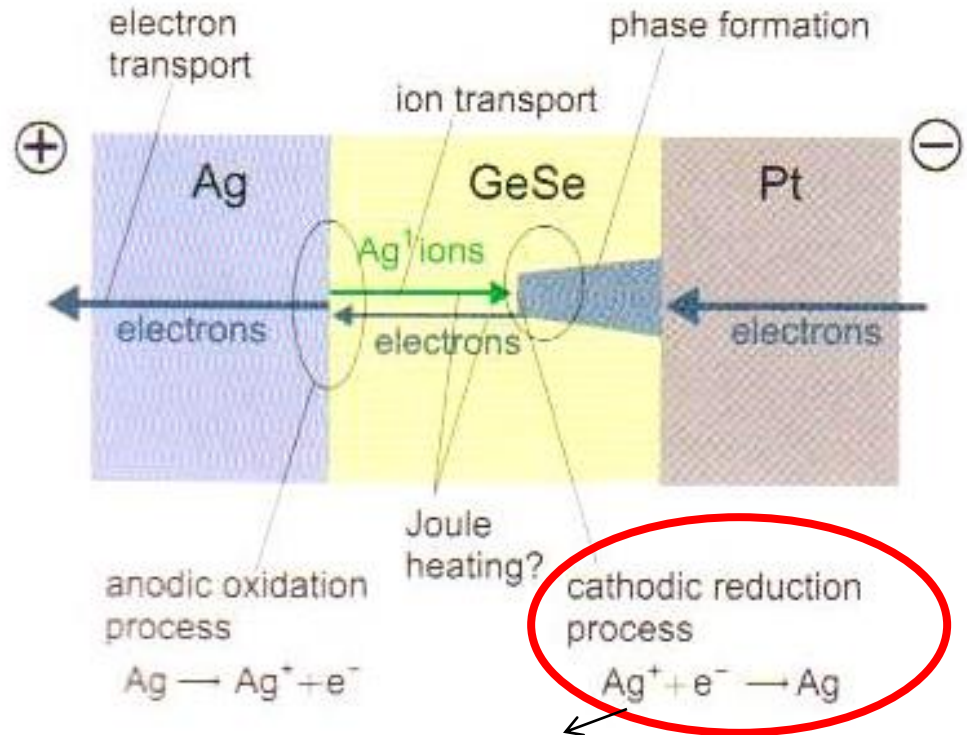


SET Process

- (a) Anodic oxidation and dissolution of M:
 $M \rightarrow M^{z+} + ze^-$
- (b) Migration of M^{z+} across thin film
 (migrations is strongly enhanced by extended defects)
- (c) Reduction and electro-crystallization of M on the surface of CE:



- Formation of filament growing (typically) in the direction of the active electrode.
- A forming step (first sweep) is required
- The growth is limited by current compliance



Origin of Non-linearity

Butler-Volmer equation for oxidation reductions

- Exponential for high overpotentials

$\Delta\phi$ ~ applied potential
 α : cathodic charge transfer coef.

$$J = J_0 \left[\exp \left(\frac{(1-\alpha)ze}{k_B T} \Delta\phi \right) - \exp \left(-\frac{\alpha ze}{k_B T} \Delta\phi \right) \right]$$

Ox(ide)RAM (redox based)

OxRAM is typically a transition metal oxide sandwiched between inert electrodes

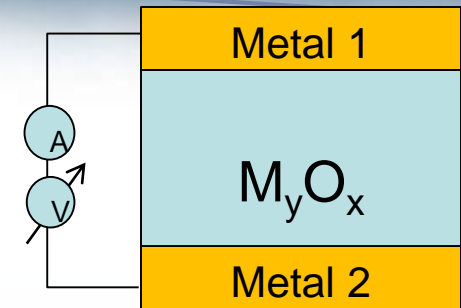
(no metal cations available as in ECM).

If a sufficient voltage (or current) stress is applied, the insulating material can become conductive

Two distinct I-V switching phenomena are reported

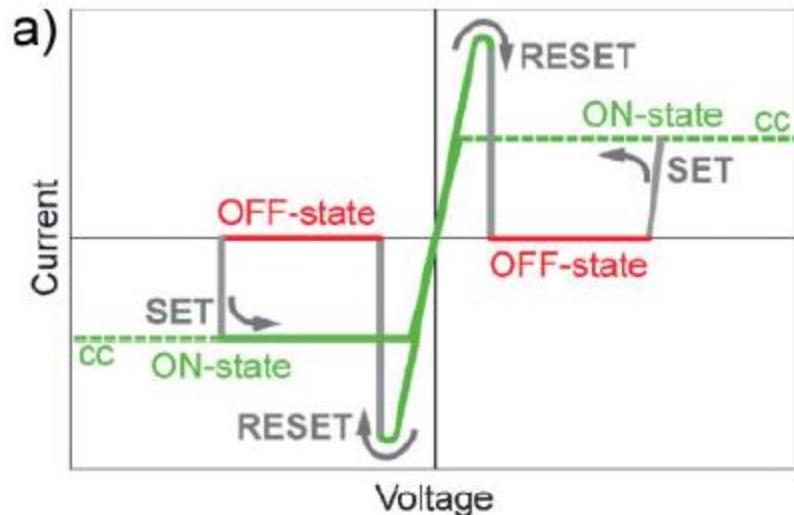
Unipolar: The same polarity can tune ON and OFF the cell

Bipolar: One polarity switch ON, the other switch OFF



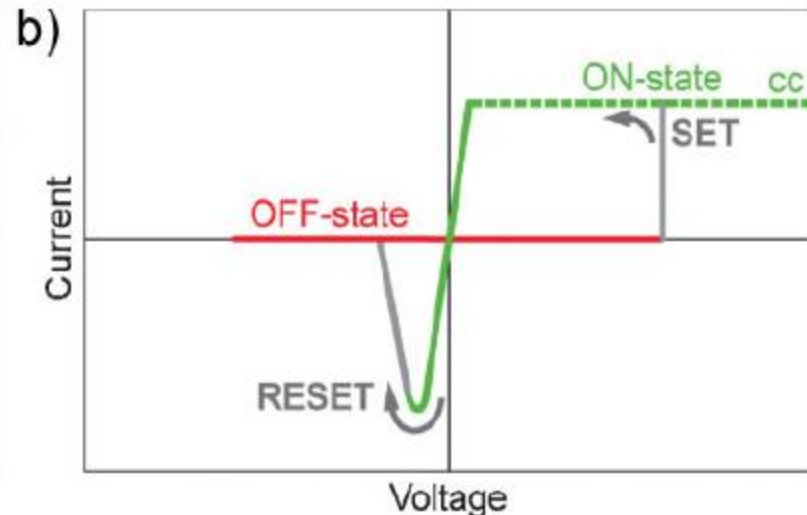
“Thermo Chemical Memory”

UNIPOLAR



“Valence Change Memory”

BIPOLAR



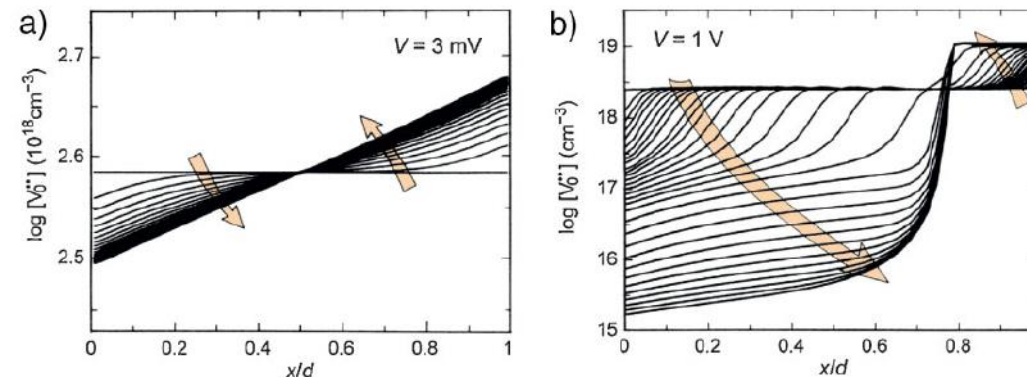
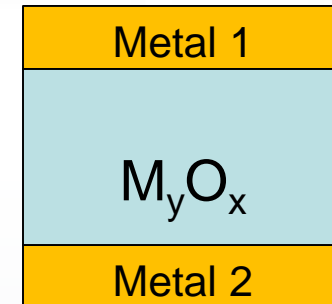
Valence Change Memory (redox-based)

In TMO, oxygen vacancies (V_O^{2+}) are much more mobile than cations.

This has been evidenced by coloration measurement in slightly doped oxide crystal

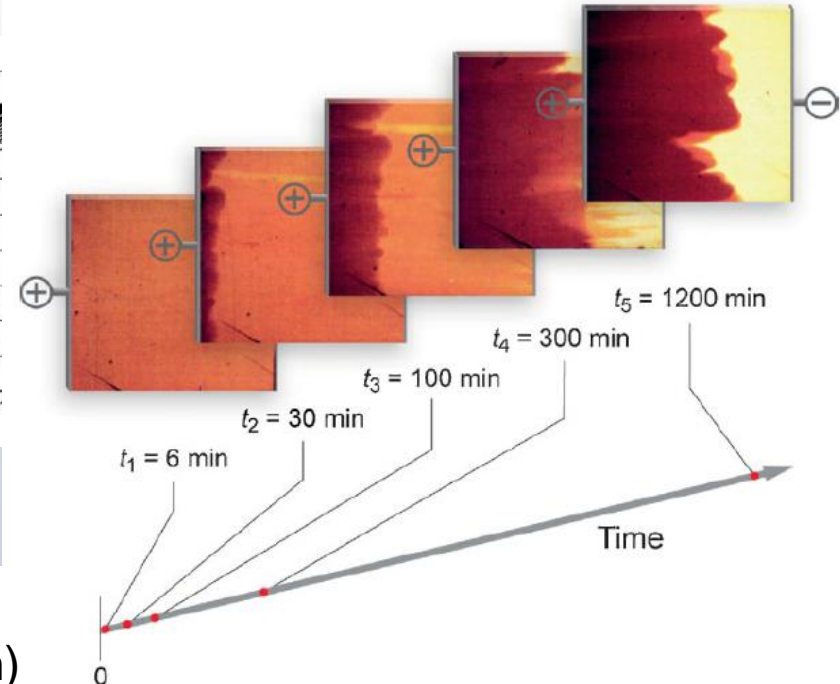
The doping vision (in crystal):

By changing the V_O^{2+} distribution, two doping regions can be formed, n and p respectively. For highly doped TMO, the n-type can become highly conductive



Slightly Fe doped STO

Red: Fe^{4+} , p-type region
White: Fe^{3+} , n-type region (V_O rich)



Valence Change Memory (redox-based)

In the case of thin films, the TMO are most of the time amorphous. But still, the V_O^{2+} are expected to be the mobile species (no direct evidence of V_O^{2+} migration in amorphous TMO)

The stoichiometry vision :

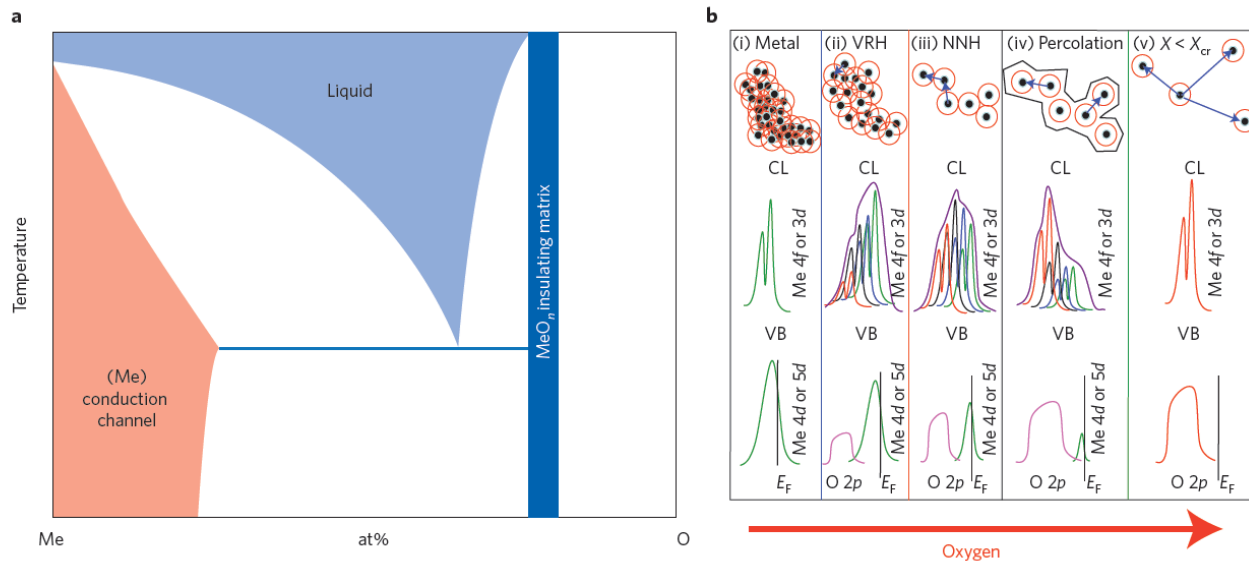
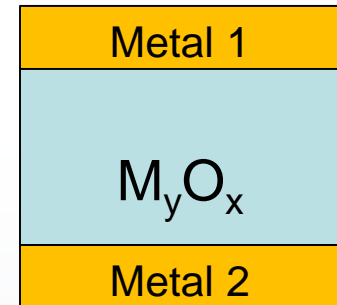
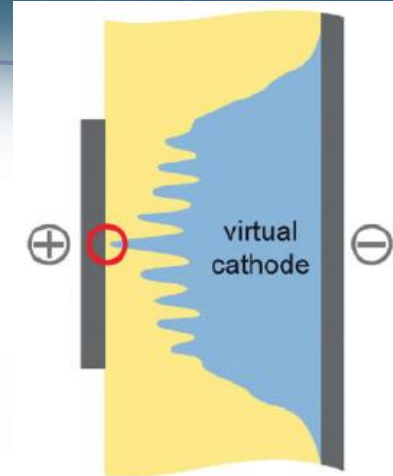
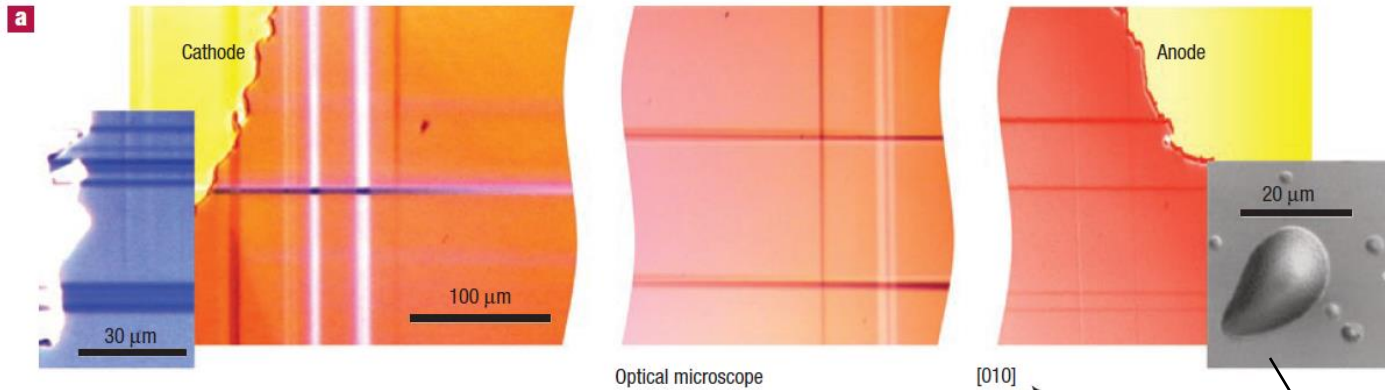


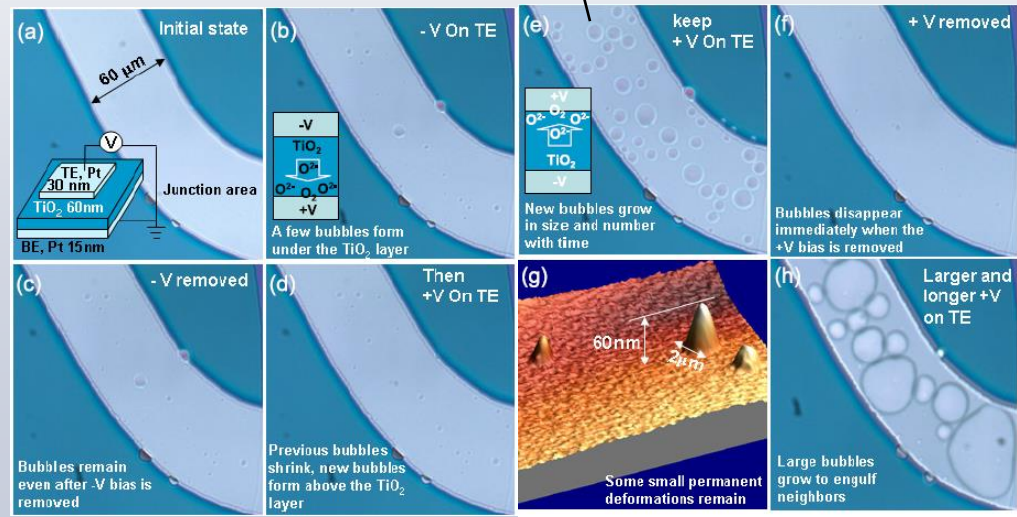
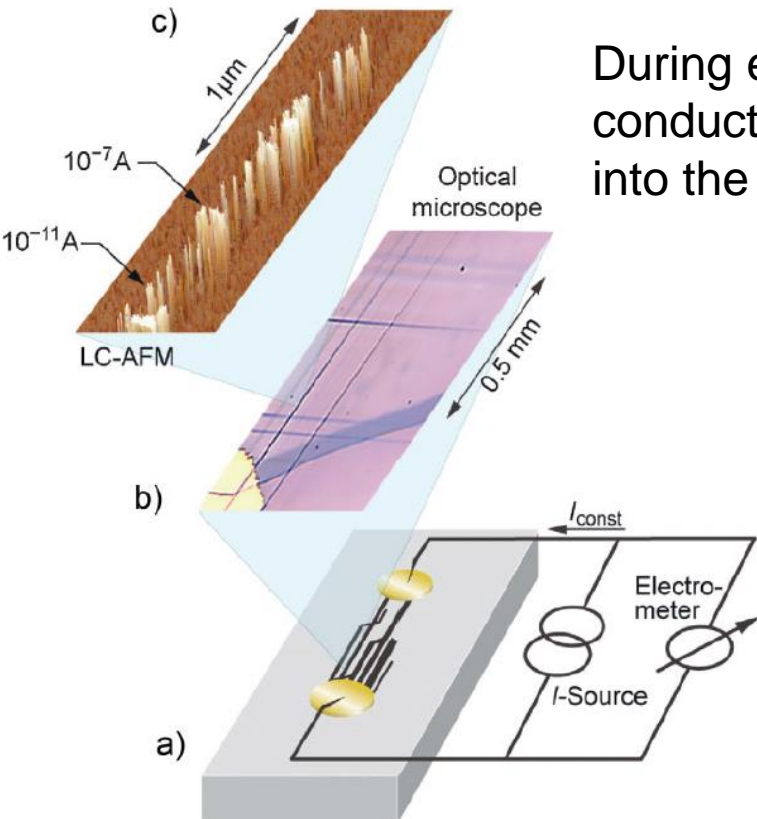
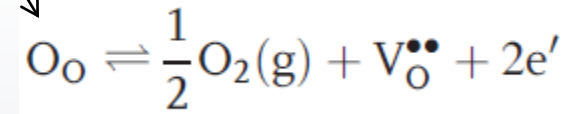
Figure 2 | Material selection criteria for high endurance and repeatability. **a**, Simplified schematic phase diagram of a metal-oxygen (Me-O) system with only two solid-state phases at low temperature. The MeO_n phase is an insulating stoichiometric phase, serving as the matrix material in the switching device illustrated schematically in Fig. 1. The (Me) phase is a metal-oxygen solid solution, serving as the conduction channel. These two phases are thermodynamically stable with each other and do not mix by reaction to form an intermediate phase even at high temperature, for example, locally induced by Joule heating. The metal (Me) has a large solubility of oxygen, readily accommodating mobile oxygen anions or vacancies during switching. **b**, With increasing oxygen content in the channel region, the electron transport mechanism changes, producing corresponding resistance changes. The schematic depicts a sequence of evolving conduction centre density and conduction mechanisms (top), and corresponding photoemission core-level (CL, middle) and valence-band (VB, bottom) measurements, from a disordered transition metal oxide in the course of oxidation. The red circles are the localization radii. Unoxidized metallic state (i), weakly localized variable range hopping (VRH) regime (ii), more strongly localized nearest-neighbour hopping (NNH, iii), strong localization regime on the verge of percolation breakdown (iv), and final highly insulating sub-percolation insulating state (v). X is the fraction of conduction centre sites and X_{cr} is the critical fraction at the percolation threshold. E_F , Fermi energy. Panel **b** reproduced with permission from ref. 73, © 2012 Springer.

| Insulators | Bottom Electrode | Top electrode | Switching mode | reference |
|----------------------------------------------------------------------------|----------------------------------------|---------------|--------------------|-----------|
| MgO | Pt | Pt | Unipolar | 1 |
| TiO _x | Ru, Pt | Al, Pt | Non/Uni/Bipolar | 2, 3 |
| ZrO _x | P ⁺ -Si, n ⁺ -Si | Pt, Cr | Uni/Bipolar | 4-6 |
| HfO _x | TiN | TiN | Bipolar | 7 |
| VO _x | N/A | N/A | Threshold | 8, 9 |
| NbO _x | P ⁺ -Si | Pt | Unipolar | 10 |
| TaO _x | Pt, Ta | Pt, Ta | Bipolar | 11, 12 |
| CrO _x | TiN | Pt | Bipolar | 13 |
| MoO _x | Pt | Pt-Ir | Uni/Bipolar | 14 |
| WO _x | W, FTO | TiN, Au | Bipolar | 15, 16 |
| MnO _x | Pt | Al, TiN | Bipolar | 17, 18 |
| FeO _x | Pt | Pt | Non/Bipolar | 19, 20 |
| CoO _x | Pt | Pt | Nonpolar | 21 |
| NiO _x | Pt | Pt | Nonpolar/Threshold | 22, 23 |
| CuO _x | TiN, TaN, SRO, Pt | Pt | Bipolar | 24 |
| ZnO _x | Pt, Au | TiN, Ag | Bipolar | 25-27 |
| AlO _x | Ru, Pt | Pt, Ti | Unipolar/Bipolar | 28, 29 |
| GaO _x | ITO | Pt, Ti | Bipolar | 30 |
| SiO _x | Poly-Si, TiW | Poly-Si, TiW | Unipolar | 31 |
| SiO _x N _y | W | Cu | Bipolar | 32 |
| GeO _x | ITO, TaN | Pt, Ni | Bipolar | 33, 34 |
| SnO ₂ | Pt | Pt | Unipolar | 35 |
| BiO _x | Bi | W, Re, Ag, Cu | Bipolar | 36 |
| SbO _x | Pt | Sb | Unipolar/Bipolar | 37 |
| SmO _x | TiN | Pt | Bipolar | 38 |
| GdO _x | Pt | Pt | Unipolar | 39 |
| YO _x | Al | Al | Unipolar | 40 |
| CeO _x | Pt | Al | Bipolar | 41 |
| EuO _x | TaN | Ru | Uni/Bipolar | 42, 43 |
| PrO _x | TaN | Ru | Bipolar | 42, 43 |
| ErO _x | TaN | Ru | Unipolar | 42, 43 |
| DyO _x | TaN | Ru | Unipolar | 42, 43 |
| NdO _x | TaN | Ru | Unipolar | 42, 43 |
| Ba _{0.7} Sr _{0.3} TiO ₃ | SrRuO ₃ | Pt, W | Bipolar | 44 |
| SrTiO ₃ | SrRuO ₃ , Au, Pt | Au, Pt | Bipolar | 45 |
| SrZrO ₃ | SrRuO ₃ | Au | Bipolar | 46 |
| BiFeO ₃ | LaNiO ₃ | Pt | Bipolar | 47 |
| Pr _{0.7} Ca _{0.3} MnO ₃ | YBCO, Pt, LaAlO ₃ | Ag | Bipolar | 48 |
| La _{0.33} Sr _{0.67} FeO ₃ | Au | Al | Bipolar | 49 |
| Pr _y La _{0.625-y} Ca _{0.375} MnO ₃ | Ag | Ag | Bipolar | 50 |
| Nitrides (AlN) | Al, TiN, Pt | Al, TiN, Pt | Bipolar | 51 |
| Telluride (ZnTe) | Si | Au | Bipolar | 52 |
| selenide (ZnSe) | P ⁺ -Ge | In, In-Zn | Bipolar | 53 |
| Polymers | Al, ITO, Cu | Al, ITO, Cu | Bipolar | 54, 55 |

Electroforming (cristal)



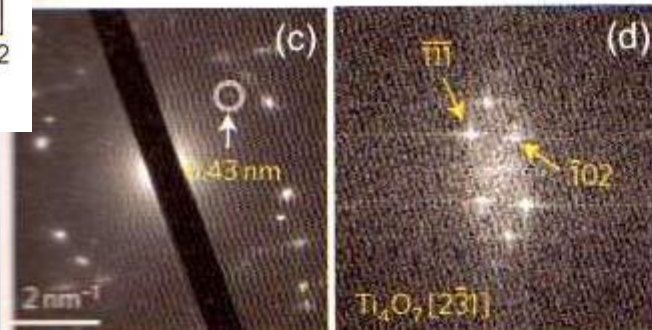
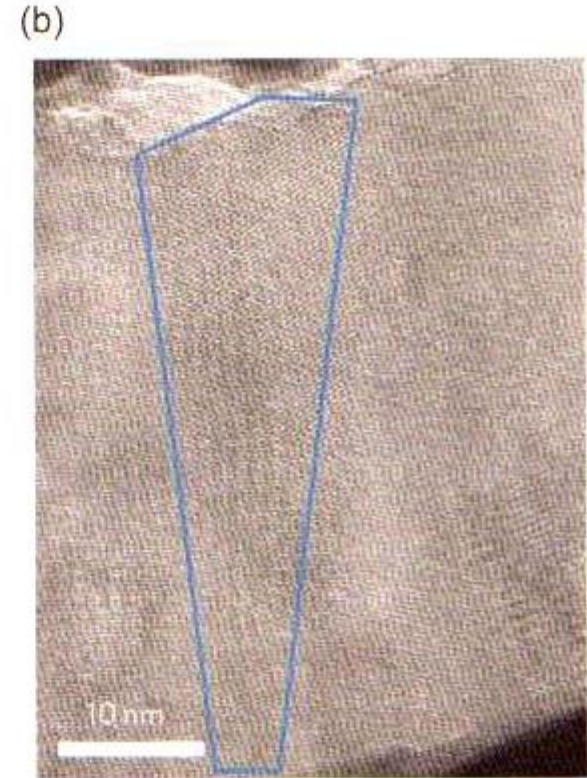
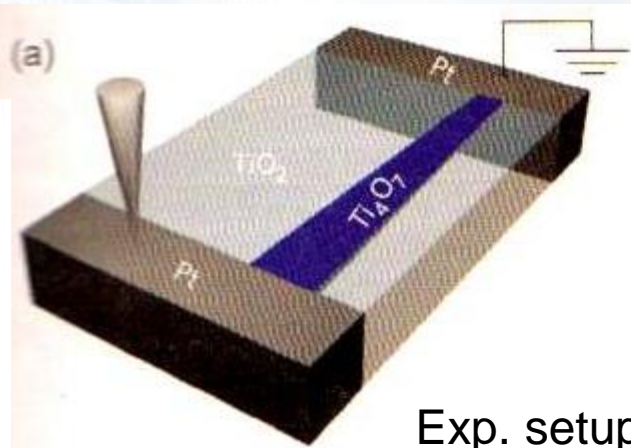
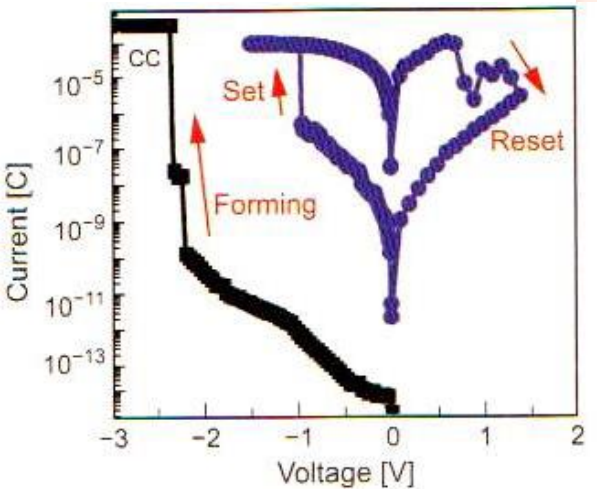
During electroforming, conducting filament are created into the oxide.



Electroforming (thin film)

Observation of Magneli phases in TiO_2

Example of forming



X ray-diffraction

TEM image

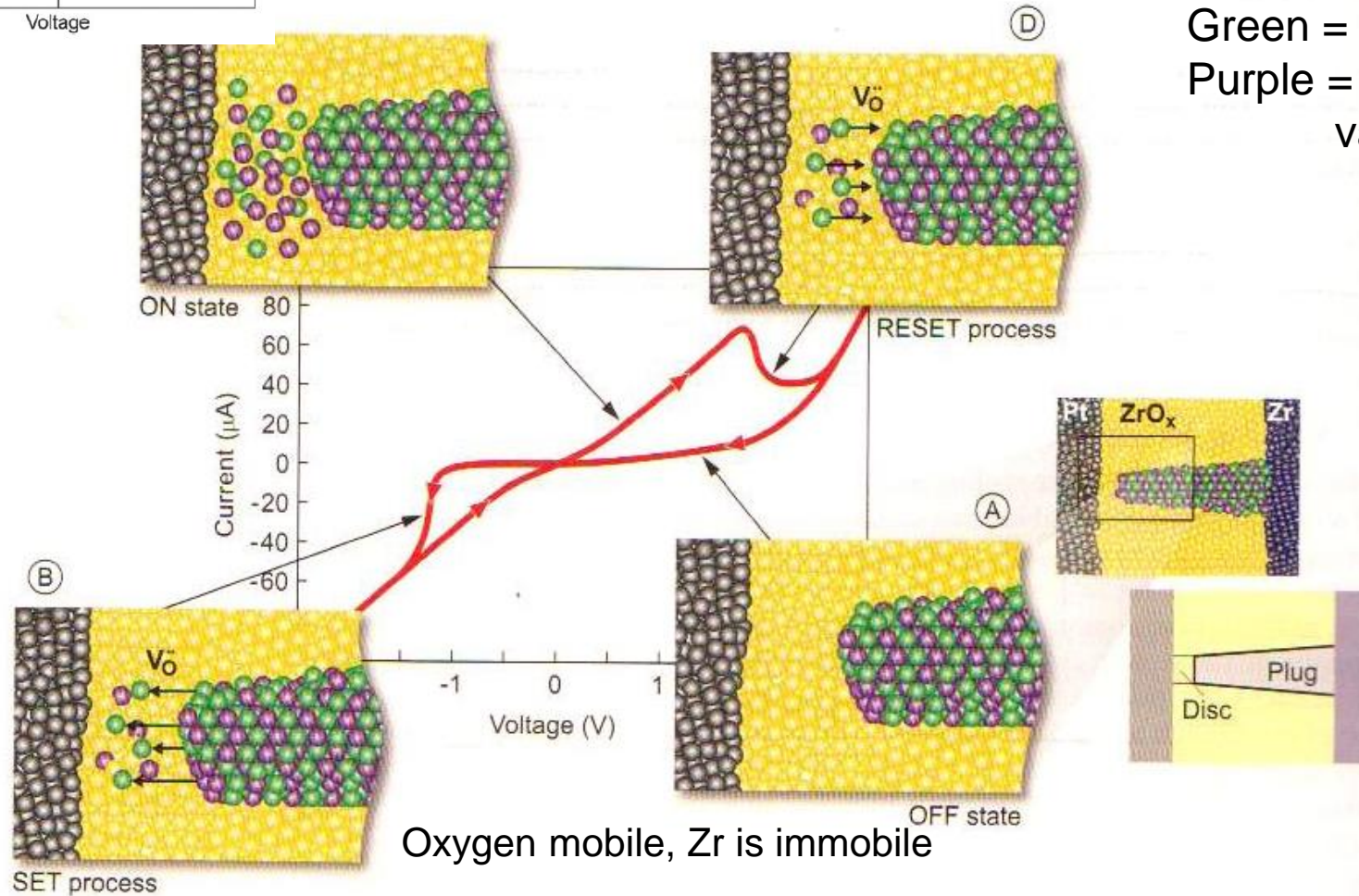
- Forming is thermally assisted and two step process (reduction and migration)

b)



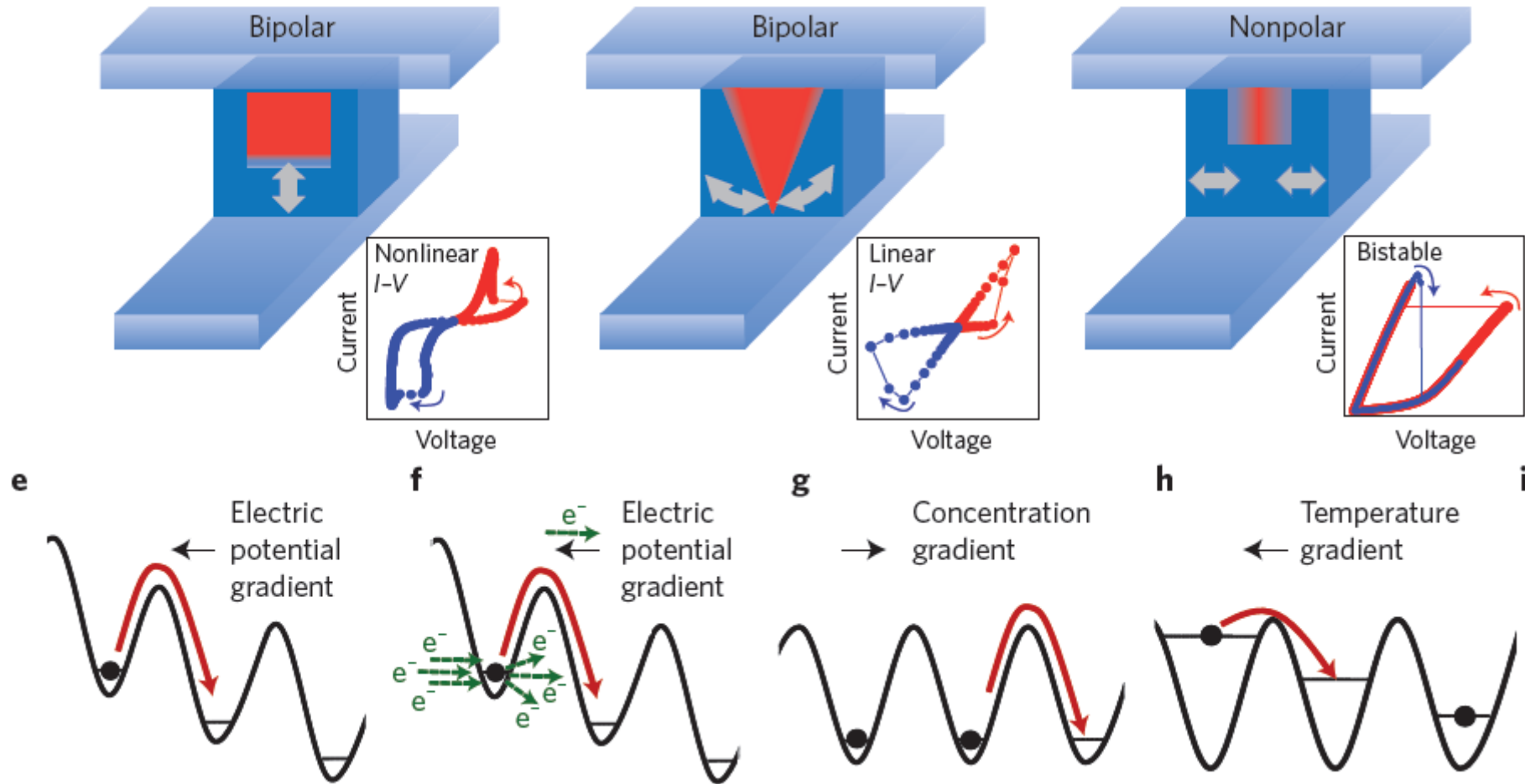
Pt/ZrO_x/Zr

Green = O
Purple = Zr in lower valence state



Oxygen mobile, Zr is immobile

Mechanism for switching



Practically, even if one mechanism is more important, switching results from a combination

Non linearity

$$\mu_{V_0} = \frac{z_{V_0} e_0}{kT} D_0 \exp(-W_D/kT)$$

Vacancies mobility increase exponentially with temperature

Other factor:

- Maybe the stability of the two phases (i.e. stoichiometric vs high $V_{O^{2+}}$ concentration)

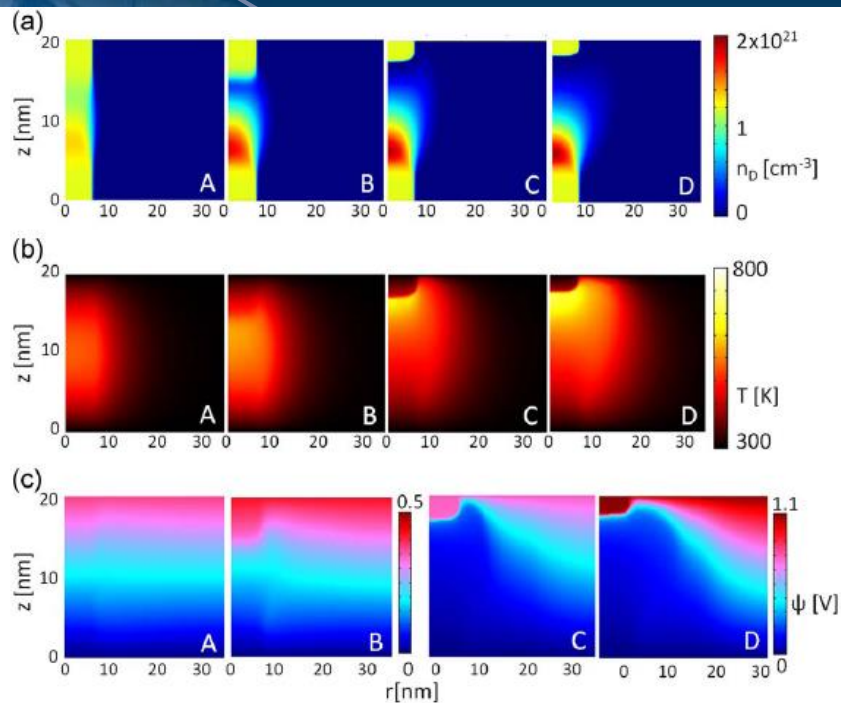
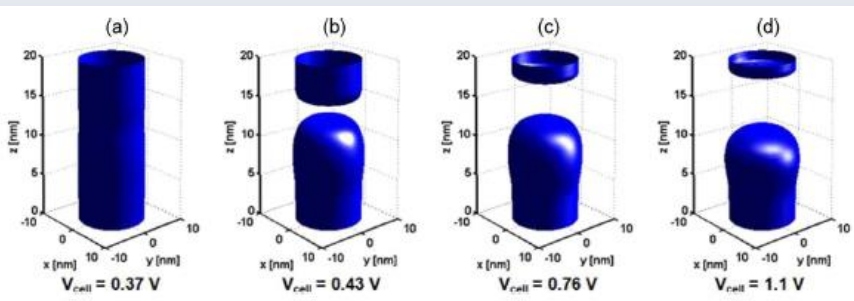
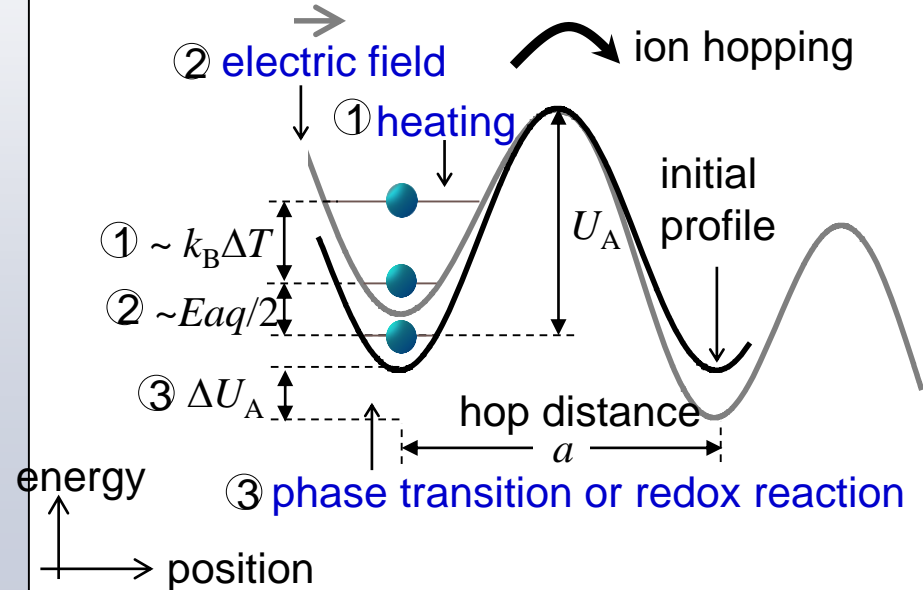


Fig. 5. Calculated map of (a) dopant density n_D , (b) T , and (c) potential ψ for bias points A, B, C, and D along the reset sweep in Fig. 4(a). Calculations are shown as a function of radial coordinate r and vertical coordinate z according to Fig. 1.



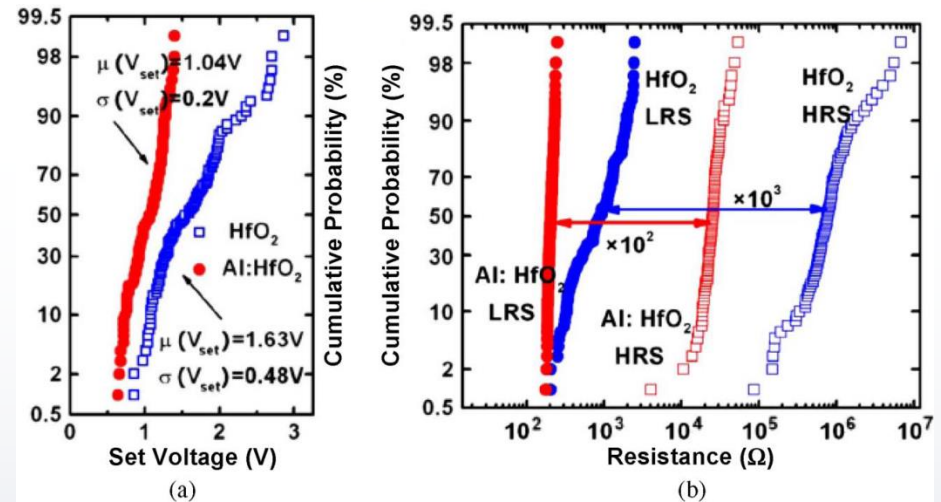
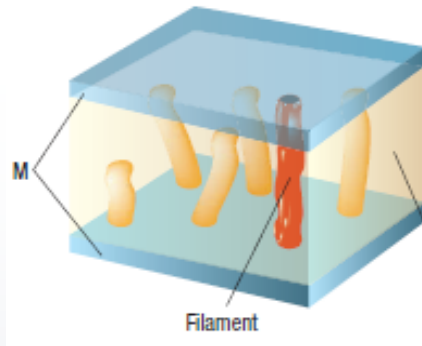
barrier modulation due to:



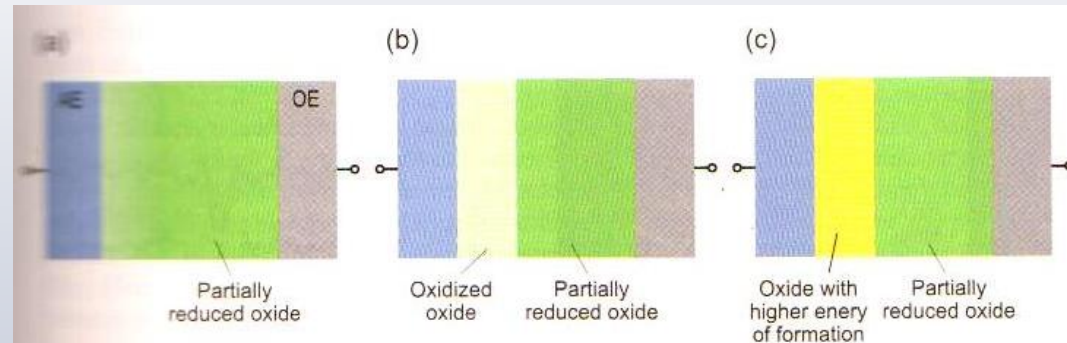
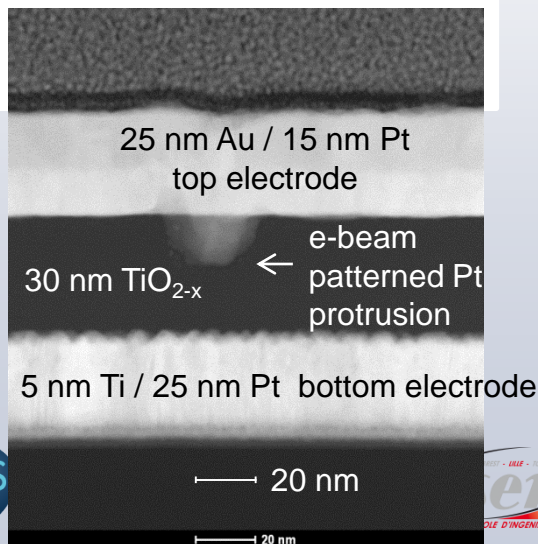
RRAM Challenges

Main challenge: deal with dispersion

Because forming is stochastic, dispersion in switching properties are huge



Solution: towards forming free devices



AE = active electrode (low oxygen affinity, high work function, e.g Pt, Ir, TiN)
OE = Ohmic electrode (opposite, e.g Ti, Ta)

- (a) Homogeneous monolayer, e.g. TiO_{2-x} – forming is crucial
- (b) Homogeneous bi-layer, e.g. TiO₂/TiO_{2-x} or Ta₂O₅/TaO_x
- (c) Heterogeneous bi-layer, e.g. Al₂O₃/TiO_{2-x} or HfO₂/TiO_{2-x}

RRAM Challenges

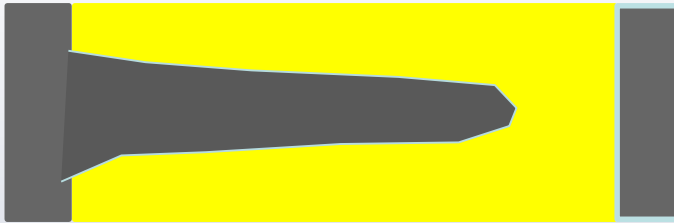
Main challenge: energy consumption

Lowest E/Bit reported is few pJ. Ideally, we want to go to the sub pJ regime

Solution: filament engineering

Trade off between filament resistance and ON/OFF ratio. (Need to increase the resistance of the filament)

High conductivity (metallic filament)



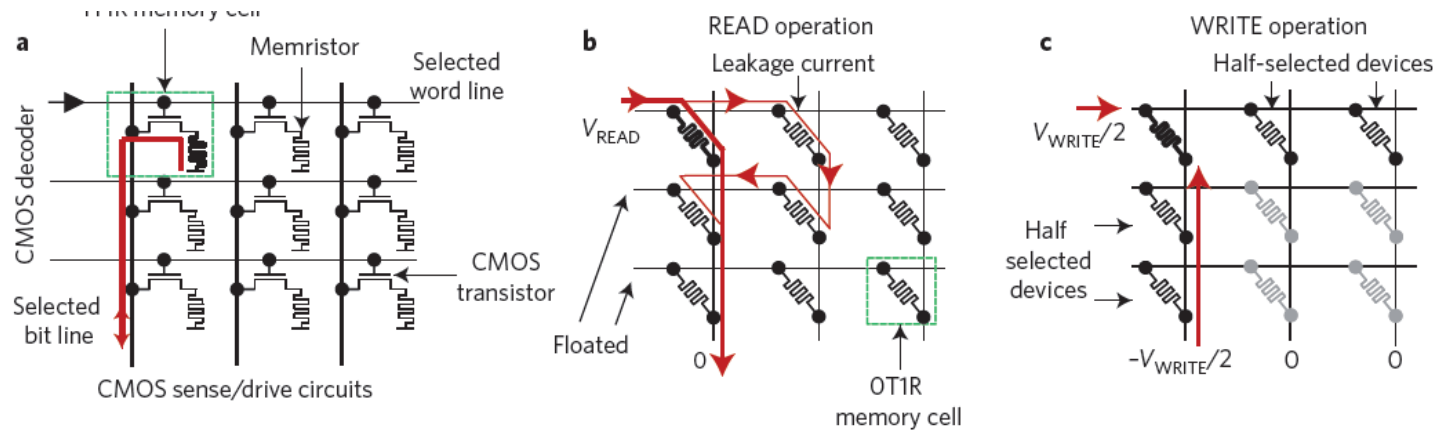
Moderate conductivity (Semi-metallic)



- Scaling of the filament
- Control of defects in the filament (i.e. control of conductivity)

RRAM challenges

Main challenge: high density crossbar implementation



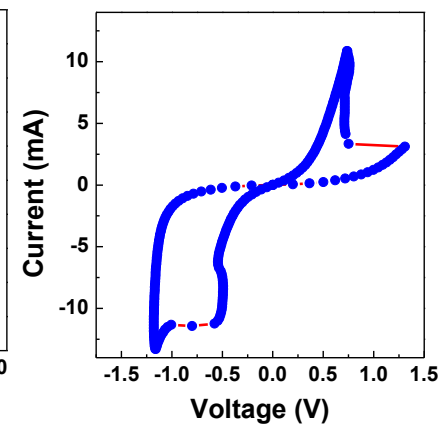
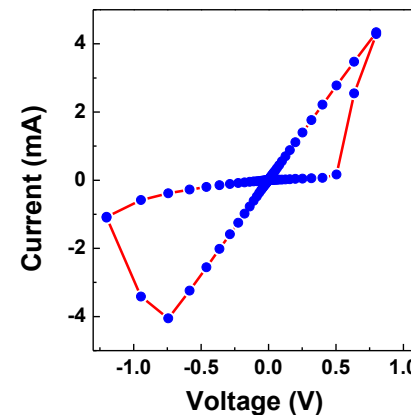
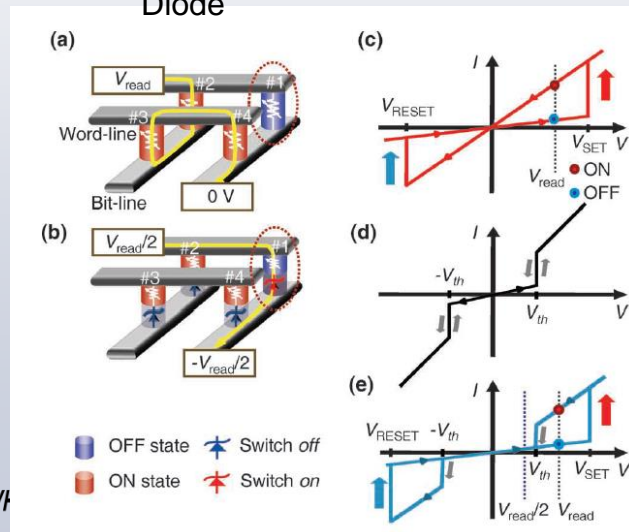
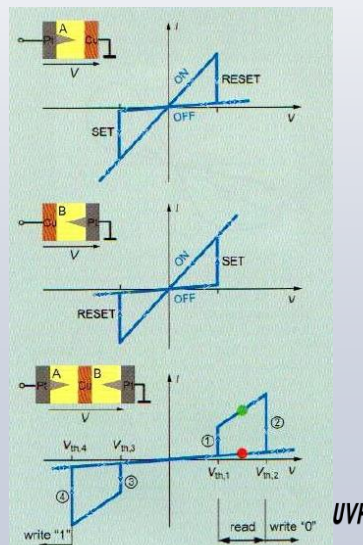
Additional challenges: Nanowire resistance contribution and high current effect on wire during operation

Solutions:

Complementary switching

Selector device:
Tunnel junction
S type
Diode

Intrinsic non-linear I-V





Thanks for your attention